77N 31175

NASA TECHNICAL MEMORANDUM

NASA TM-73,254
(Revised 8/30/78)

NASA TM-73,254

A MATHEMATICAL FORCE AND MOMENT MODEL OF A UH-1H HELICOPTER FOR FLIGHT DYNAMICS SIMULATIONS

Peter D. Talbot and Lloyd D. Corliss

Ames Research Center, NASA

and

Ames Directorate, USAAMRDL, AVRADCOM
Ames Research Center
Moffett Field, Calif. 94035

June 1977

NOTATION

a	main rotor lift curve slope, per radian
a_o	main rotor coning, rad
a_1, b_1	first harmonic values of main rotor blade flapping with respect to control axis, rad
a_{1s}, b_{1s}	first harmonic values of main rotor blade flapping with respect to shaft axis, rad
a_{1sw}	longitudinal component of control axis position, rad
A	rotor disk area, πR^2, ft^2, m^2
$A_{x,y,z}$	body axis accelerations, ft/sec^2, m/sec^2
A_{1C}	lateral swashplate control input, rad
A_{1CB}	lateral cyclic pitch contribution of stabilizer bar, rad
A_{1CL}	lateral swashplate control bias rigging term, rad
A_{1CP}	lateral pilot control input, rad
A_{1s}	lateral control axis command position with respect to shaft, rad
b_{1sw}	lateral component of control axis position, rad
B_{1C}	longitudinal swashplate control input, rad
B_{1CB}	longitudinal cyclic pitch contribution of stabilizer bar, rad
B_{1CL}	longitudinal swashplate control bias rigging term, rad
B_{1CP}	longitudinal pilot control input, rad
B_{1S}	longitudinal control axis command position with respect to shaft, rad
C_1, C_4	constants in linkage equations, cyclic stick to swashplate motion, rad/in., rad/cm
C_5	constant in linkage equation, collective pitch to collective stick motion, rad/in., rad/cm
C_6, C_7	constants in linkage equation, tail rotor collective pitch to pedal motion, rad/in., rad/cm

D	main rotor diameter, ft, m
D_1, D_2, D_3	constants in fuselage drag force equations, $lb/(ft/sec)^2$, $N/(m/sec)^2$
fe_1, fe_2, fe_3	drag areas of fuselage, ft^2, m^2
F_1	vertical fin drag constant, $lb/(ft/sec)^2$, $N/(m/sec)^2$
G_1	constant used in ground effect computation
$\dot{h}$	helicopter rate of climb
h_{TR}	height of tail rotor above c.g., ft, m
H	rotor H-force in control axis - wind system, lb, N
H_1, H_2, H_4	constants in horizontal stabilizer aerodynamic forces, $lb/(ft/sec)^2$, $N/(m/sec)^2$
$I_{xx}, I_{yy}, I_{zz}, I_{xz}$	inertias in body axis
k_1, k_2	constants in vertical fin aerodynamic forces, $lb/(ft/sec)^2$, $N/(m/sec)^2$
K_B	numerator term, combining linkage and damping constants, of stabilizer bar input to cyclic pitch, sec
K_G	constant in λ equation representing ground effect
ℓ_H	waterline displacement of rotor hub from aircraft center of gravity, ft, m
ℓ_{HS}	longitudinal displacement of horizontal stabilizer aerodynamic center from aircraft center of gravity, ft, m
ℓ_{TR}	longitudinal displacement of tail rotor hub from aircraft center of gravity, ft, m
ℓ_{VF}	waterline displacement of vertical fin aerodynamic center from aircraft center of gravity, ft, m
L_1	constant in fuselage aerodynamic force contribution, $lb/(ft/sec)^2$, $N/(m/sec)^2$
L_R	body axis rolling moment, due to main rotor, ft-lb, J
L_{TR}	body axis rolling moment, due to tail rotor, ft-lb, J
M_1	constant in fuselage aerodynamic pitching moment, $ft\text{-}lb/(ft/sec)^2$, $J/(ft/sec)^2$

M_F	body axis pitching moment, due to fuselage, ft-lb, J
M_H	body axis pitching moment, due to horizontal stabilizer, ft-lb, J
M_R	body axis pitching moment, due to main rotor, ft-lb, J
N_1	constant in fuselage aerodynamic yawing moment, ft-lb/(ft/sec)^2, J/(m/sec)^2
N_F	body axis yawing moment, due to fuselage, ft-lb, J
N_R	body axis yawing moment, due to main rotor, ft-lb, J
N_{TR}	body axis yawing moment, due to tail rotor, ft-lb, J
N_{VF}	body axis yawing moment, due to vertical fin, ft-lb, J
p_B	body axis roll rate, rad/sec
p_C	main rotor shaft roll rate, wind-control axis system, rad/sec
Q	main rotor torque, ft-lb, J
q_B	body axis pitch rate, rad/sec
q_C	main rotor shaft pitch rate, wind-control axis system, rad/sec
r_B	body axis yaw rate, rad/sec
R	rotor radius, ft, m
$R_1,R_2,...R_9$	constants in main rotor force equations, table 3
(s)	Laplace operator
S	area of aerodynamic surface, ft^2, m^2
T	main rotor thrust, lb, N
$T_1,T_2,...T_5$	constants in tail rotor force equations, table 3
T_{TR}	tail rotor thrust, lb, N
u_B	x-body axis relative velocity, ft/sec, m/sec
u_C	longitudinal component of relative wind in wind control axis system, ft/sec, m/sec
u_F	component of relative wind in equations for vertical fin aerodynamic force, ft/sec, m/sec

u_H	component of relative wind in equations for horizontal stabilizer aerodynamic force, ft/sec, m/sec
v_B	y-body axis relative velocity, ft/sec, m/sec
v_C	lateral component of relative wind in wind-control axis system, ft/sec, m/sec
v_F	component of relative wind in equations for vertical fin aerodynamic force, ft/sec, m/sec
v_T	relative wind normal to plane of tail rotor, ft/sec, m/sec
w_B	z-body axis relative velocity, ft/sec, m/sec
w_C	vertical component of relative wind in wind-control axis system, ft/sec, m/sec
w_H	component of relative wind in equations for horizontal stabilizer aerodynamic force, ft/sec, m/sec
X_C	main rotor force in control axis system, lb, N
X_F	longitudinal x-body force, due to fuselage, lb, N
X_R	longitudinal x-body force, due to main rotor, lb, N
$X_{c.g.}$	longitudinal distance of aircraft center of gravity forward of main rotor shaft hub, ft, m
Y	rotor Y-force in wind control axis system, lb, N
Y_1	constant in fuselage aerodynamic force contribution, lb, N
Y_C	main rotor force in control axis system, lb, N
Y_F	lateral y-body force, due to fuselage, lb, N
Y_R	lateral y-body force, due to main rotor, lb, N
Y_{TR}	lateral y-body force due to tail rotor, lb, N
Y_{VF}	lateral y-body force, due to vertical fin, lb, N
Z	rotor height above ground plane, ft, m
Z_C	main rotor force in control axis system, lb, N
Z_F	vertical z-body force, due to fuselage, lb, N

Z_H — vertical z-body force, due to horizontal stabilizer, lb, N

Z_R — vertical z-body force, due to main rotor, lb, N

α_F — vertical fin angle of attack, rad

α_{HS} — horizontal stabilizer angle of attack, rad

β_m — maximum flapping amplitude of main rotor with respect to shaft, rad

γ — rotor Lock number for one blade, $\rho \frac{aCR^4}{I_\beta}$

δ — rotor mean blade drag coefficient

δ_o, δ_2 — constants in rotor drag equation

δ_{1B}, δ_{2B} — stabilizer bar flapping constants, rad

δ_a — pilot's lateral stick displacement, in., cm

δ_c — pilot's collective stick displacement, in., cm

δ_e — pilot's longitudinal stick displacement, in., cm

δ_p — pilot's pedal displacement, in., cm

δ_s — horizontal stabilizer incidence angle, rad

θ — aircraft pitch attitude Euler angle, deg, rad

θ_o — main rotor collective pitch

θ_{TR} — tail rotor collective pitch, rad

λ — main rotor inflow ratio

μ — main rotor advance ratio

ρ_o — sea level air density, slugs/ft^3, kg/m^3

σ — rotor solidity

τ_B — stabilizer bar time constant, sec

τ_R — control axis response time constant, sec

ϕ — aircraft roll attitude, rad

ϕ_c — amplitude of total cyclic pitch control input, rad

ϕ_p — phase angle of cyclic rigging, deg

ϕ_t	phase (with respect to body axis) of total cyclic pitch control input, rad
ψ	aircraft heading, rad
Ω	rotor rational speed, rad/sec

Subscripts

TR	tail rotor
VF	vertical fin
HS	horizontal stabilizer
IC	initial conditions - trimmed conditions for the helicopter
m	model

A MATHEMATICAL FORCE AND MOMENT MODEL OF A UH-1H HELICOPTER FOR FLIGHT DYNAMICS SIMULATIONS

Peter D. Talbot and Lloyd D. Corliss

Ames Research Center, NASA
and
Ames Directorate, USAAMRDL, AVRADCOM

SUMMARY

A model of a Bell UH-1H helicopter was developed to support several simulations at Ames Research Center and was used also for development work on an avionics system known as the V/STOLAND system at Sperry Flight Systems. This report presents the complete equations and numerical values of constants used to represent the helicopter.

Responses to step inputs of the cyclic and collective controls are shown and compared with flight test data for a UH-1H. The model coefficients were adjusted in an attempt to get a consistent match with the flight time histories at hover and 60 knots. Fairly good response matching was obtained at 60 knots, but the matching at hover was not as successful. Pilot evaluations of the model, both fixed and moving base, were made.

INTRODUCTION

The mathematical force and moment model described was developed to satisfy the need for representing the dynamics of a UH-1H helicopter for piloted simulation. The model was developed specifically for use in flight dynamics investigations and for simulation of terminal-area guidance and navigation tasks. It has been used in simulations for the development of software for the navigation and guidance programs of an avionics system known as V/STOLAND and for the investigation of the effects of failures of stability augmentation elements of the control system (see ref. 1).

The equations, representing the nonlinear contributions of the components of the helicopter to the force and moments were assembled from many sources. The equations are in general form so that changes can be made to represent helicopters other than the UH-1H. The model employs a quasi-static main rotor representation, uniform inflow over the rotor disc, and simple expressions for the contributions of the tail rotor, fuselage, and empennage. No interference effects between components were modelled. In the simulation, the equations were used in a standard digital program, partially described in reference 2 which incorporates the equations of motion, variations in the atmosphere, and routines for interfacing with analog equipment for driving instruments, providing control forces, etc. Simulations have been conducted with an EAI 8400 computer.

The model was evaluated by comparing its response to step inputs with those obtained in flight on a UH-1H helicopter, and subjective pilot assessments. The pilot evaluations were obtained during both fixed and moving-base simulations.

HELICOPTER FORCE AND MOMENT EQUATIONS

The quasi-static main rotor equations were adapted from reference 3. The equations for the aerodynamic forces of the fuselage and empennage were separately derived, based either on available wind tunnel data of reference 4 or standard textbook wing theory, modified to approximate stalled conditions. An approximate representation for the tail rotor was derived; however, in its original form it did not correctly predict tail rotor damping. The form of the equations was retained with adjusted constant values used to match the apparent tail rotor damping seen in the flight test data yaw responses.

The equations represent aerodynamic forces and moments contributed by each component of the helicopter. The net results are three aerodynamic forces and three aerodynamic moments applied in a body-axis system. The origin of the body system is the helicopter c.g. The z axis of the reference frame was taken to be parallel to the main rotor shaft, positive direction down, as in figure 1.

The constant values used for the coefficients in the equations are presented in tables 1 and 2. It may be noted that the characteristic lengths used to compute moments are based on data referenced to the waterline-buttline-station system of the helicopter, rather than the axis system defined above. Since the UH-1H has a 5° forward mast tilt, slight discrepancies are introduced by using raw station and waterline values to locate components of the model. These are thought to be insignificant.

Main Rotor Forces at the Rotor Hub

$$T = R_1\left[\theta_o\left(\frac{1}{3} + \frac{\mu^2}{2}\right) + \frac{\lambda}{2} + R_2\mu p_C\right] \tag{1}$$

$$\begin{aligned} H = R_1\Bigg\{ & R_3\delta\mu + a_1\left[\frac{\theta_o}{3} + \frac{3}{4}\lambda\left(1 - \frac{3}{8}\mu^2\right) + \frac{\mu a_1}{4}\right] - \frac{\mu\lambda\theta_o}{2}\left(\frac{1 - 2\mu}{3\pi}\right) - \frac{\lambda^2\mu}{4} \\ & - \frac{3}{8}\lambda\mu^2(1 + 3.33\mu) - a_o\left(\frac{b_1}{6} - \frac{a_o\mu}{4}\right) - R_4 q_C\left(\frac{a_o}{6} + \frac{\mu b_1}{16}\right) \\ & - R_4 p_C\left(\frac{\theta_o}{6} + \frac{\lambda}{2}\right) + \frac{\mu a_1}{16}\Bigg\} \end{aligned} \tag{2}$$

$$Y = R_1\left\{a_o\left[a_1\left(\frac{1}{6} - \mu^2\right) - \frac{3}{2}\mu\left(\lambda + \frac{\theta_o}{2}\right)\right] + b_1\left[\frac{\theta_o}{3}\left(1 + \frac{3}{2}\mu^2\right) + \frac{3}{4}\lambda + \frac{\mu a_1}{4}\right]\right.$$

$$\left. + R_4 q_C\left(\frac{\theta_o}{6} + \frac{\lambda}{2} + \frac{7}{16}\mu a_1\right) - R_4 p_C\left(\frac{a_o}{6} - \frac{5}{16}\mu b_1\right)\right\} \tag{3}$$

Main Rotor Torque

$$Q = R_9\left[R_5\delta(1 + \mu^2) - \frac{\lambda\theta_o}{3} - \frac{\lambda^2}{2} - \frac{1}{8}\left(a_1^2 + b_1^2\right) - \frac{\mu^2}{2}\left(\frac{a_o^2}{2} + \frac{3}{8}a_1^2 + \frac{b_1^2}{8}\right)\right.$$

$$\left. - \frac{\mu\lambda a_1}{2} + \frac{\mu a_o b_1}{3}\right] \tag{4}$$

This expression was obtained from reference 5, equation (44), p. 195.

Flapping Coefficients

$$a_o = 0.048 \tag{5}$$

$$a_1 = \frac{1}{1 - \mu^2/2}\left[\mu\left(\frac{8}{3}\theta_o + 2\lambda\right) + R_4 p_C - R_6 q_C\right] \tag{6}$$

$$b_1 = \frac{1}{1 + \mu^2/2}\left(\frac{4}{3}\mu a_o - R_4 q_C - R_6 p_C\right) \tag{7}$$

Advance Ratio

$$\mu = \left(u_C^2 + v_C^2\right)^{1/2} R_7 \tag{8}$$

Mean Blade Drag Coefficient

$$\delta = \delta_o + \delta_2 T^2 \tag{9}$$

Inflow Ratio

This expression is an implicit function and required an iterative solution in the computer program.

$$\lambda = -R_7 w_C - \frac{R_8 T}{(\mu^2 + \lambda^2)^{1/2}} K_G \tag{10}$$

The K_G factor is a ground effect term and represents a reduction in inflow velocity in ground effect. The value G_1 (below) was adjusted to match performance data presented in reference 6.

$$K_G = 1 - e^{(-Z/D)/G_1} \tag{10a}$$

Wind Components at the Rotor Hub

$$u_C = -u_B - w_B B_{1S} + q_B \ell_H \tag{11}$$

$$v_C = -v_B - w_B A_{1S} - p_B \ell_H \tag{12}$$

$$w_C = -w_B + B_{1S}(u_B - q_B \ell_H) + A_{1S}(v_B + p_B \ell_H) \tag{13}$$

Rotor Forces and Moments Resolved Into Body Axes

(a) Forces in control axis system

$$X_C = \frac{Hu_C}{\left(u_C^2 + v_C^2\right)^{1/2}} + \frac{Yv_C}{\left(u_C^2 + v_C^2\right)^{1/2}} \tag{14}$$

$$Y_C = \frac{Hv_C}{\left(u_C^2 + v_C^2\right)^{1/2}} - \frac{Yu_C}{\left(u_C^2 + v_C^2\right)^{1/2}} \tag{15}$$

$$Z_C = -T \tag{16}$$

(b) Main rotor forces in body axes

$$X_R = X_C - Z_C B_{1S} \tag{17}$$

$$Y_R = Y_C - Z_C A_{1S} \tag{18}$$

$$Z_R = Z_C + X_C B_{1S} + Y_C A_{1S} \tag{19}$$

(c) Main rotor moments in body axes

$$L_R = Y_R \ell_H \tag{20}$$

$$M_R = - X_R \ell_H + Z_R X_{c.g.} \tag{21}$$

$$N_R = Q - Y_R X_{c.g.} \tag{22}$$

Pilot to Swashplate Control Equations

$$A_{1CP} = C_4 \delta_a \tag{23}$$

$$B_{1CP} = C_1 \delta_e \tag{24}$$

In this form, no cross-coupling is shown corresponding to control rigging. In the most general form,

$$A_{1CP} = C_4 \delta_a \cos \phi_p - C_1 \delta_e \sin \phi_p \tag{25}$$

$$B_{1CP} = C_4 \delta_a \sin \phi_p + C_1 \delta_e \cos \phi_p \tag{26}$$

For the UH-1H ϕ_p is actually 5°. For the simulation $\phi_p = 0°$ was used.

Main and Tail Rotor Collective Pitch

$$\theta_o(s) = \frac{C_5 \delta_c}{\tau_c S + 1} \tag{27}$$

The first order lag representation was used to match more closely the a_z acceleration data obtained from the flight test results.

$$\theta_{TR} = C_6 \delta_p + C_7 \tag{28}$$

Stabilizer Bar Transfer Functions

The Bell stabilizer bar can be represented by a simple transfer function which describes its parallel input to the cyclic pitch of the main rotor. It is characterized by a gain K_B and a time constant, τ_B, which reflect respectively the mechanical mixing ratio and the mechanical damper characteristic of the shaft-mounted bar.

$$B_{1CB}(s) = \frac{K_B}{\tau_B S + 1} q_B(s) \tag{29}$$

$$A_{1CB}(s) = \frac{-K_B}{\tau_B S + 1} p_B(s) \tag{30}$$

The bar has a pronounced effect on the stability and control characteristics of the helicopter. Values of the bar constants were obtained by consultation with Bell Helicopter Company.

Control Inputs to Cyclic Pitch

The control inputs to the rotor cyclic pitch are represented as the sum of those due to the pilot, stabilizer bar and rigging of the control system.

$$B_{1C} = B_{1CP} + B_{1CB} + B_{1CL} \tag{31}$$

$$A_{1C} = A_{1CP} + A_{1CB} + A_{1CL} \tag{32}$$

Rotor Control Axis Response to Cyclic Pitch

In this representation, A_{1C} and B_{1C} are regarded as inputs to the rotor cyclic pitch. The control axis of the helicopter is then allowed to follow with a lag related to the rotor Lock number. The terms A_{1S} and B_{1S} represent the instantaneous orientation of the control axis with respect to the fuselage body axis system (in this case, the main rotor shaft axis).

$$B_{1S}(s) = \frac{B_{1C}(s)}{\tau_R S + 1} \tag{33}$$

$$A_{1S}(s) = \frac{A_{1C}(s)}{\tau_R S + 1} \tag{34}$$

In steady state, $B_{1S} = B_{1C}$ and $A_{1S} = A_{1C}$.

Thrust T is oriented along the control axis and the H and Y forces are orthogonal to T and each other. Forces H and Y may be viewed approximately as components of the rotor force normal to the tip path plane arising from rotor tip path plane excursions from the commanded control axis position (as in ref. 7) or as unique forces derived in a consistent wind-control axis system as in reference 3. In this representation, reference 3 was followed. Equations 14 through 19 resolve the T, H and Y forces into body axes.

Control Axis Pitch and Roll Rates

In equations (1) through (7) the terms q_C and p_C are used to denote pitch and roll rates of the control axis in the control axis-wind system. They are related to the body pitch and roll rates by the following two equations:

$$p_C = -p_B \frac{u_C}{\left(u_C^2 + v_C^2\right)^{1/2}} - q_B \frac{v_C}{\left(u_C^2 + v_C^2\right)^{1/2}} \tag{35}$$

$$q_C = -q_B \frac{u_C}{\left(u_C^2 + v_C^2\right)^{1/2}} + p_B \frac{v_C}{\left(u_C^2 + v_C^2\right)^{1/2}} \tag{36}$$

Tail Rotor Thrust

$$T_{TR} = \left[-T_2 + \left(T_2^2 + T_3\left|\theta_{TR}\right|\right)^{1/2}\right]^2 \frac{\theta_{TR}}{\left|\theta_{TR}\right|}\left(1 + T_1 \frac{\left|u_B\right|}{\theta_2}\right) - \left(T_4 + T_5\left|u_B\right|\right)v_T \tag{37}$$

where

$$\theta_2 = \left|\theta_{TR}\right| \quad , \ \theta_{TR} > 0.0873$$

$$\theta_2 = 0.0873 \ , \ \theta_{TR} \leq 0.0873$$

$$v_T = v_B - r_B \ell_{TR} + p_B h_{TR} \tag{38}$$

Due to memory limitations in the computer, these equations were originally derived as an economical approximation to the tail rotor thrust of an isolated tail rotor. (The equations do not incorporate the vortex ring operating state of the tail rotor or fin interference effects.) They reflect the main influences of inflow and collective pitch on tail rotor thrust. It was found that the derivation on which T_4 was based, grossly underpredicted the tail rotor damping contribution to N_r. It was necessary, therefore, to adjust the constant empirically to match the flight test results.

Tail Rotor Contribution to Body Forces and Moments

$$Y_{TR} = T_{TR} \tag{39}$$

$$L_{TR} = Y_{TR}h_{TR} \tag{40}$$

$$N_{TR} = -Y_{TR}\ell_{TR} \tag{41}$$

Fuselage Aerodynamics

$$X_F = u_B\left(-D_1|u_B| + L_1\frac{w_B^2}{|u_B|}\right) \tag{42}$$

$$Y_F = v_B\left(-D_2|v_B| - Y_1|u_B|\right) \tag{43}$$

$$Z_F = w_B\left(-D_3|w_B| - L_1|u_B|\right) \tag{44}$$

$$M_F = M_1w_B|u_B| \tag{45}$$

$$N_F = -N_1v_Bu_B \tag{46}$$

Vertical Fin Aerodynamics

$$u_F = u_B \tag{47}$$

$$v_F = -v_B + \ell_{VF}r_B \tag{48}$$

$$\sin\alpha_F = v_F/(u_F^2 + v_F^2)^{1/2} \tag{49}$$

$$Y_{VF} = K_1v_Fu_F + F_1v_F|v_F| \qquad \begin{matrix} -20° \le \alpha_F \le 20° \\ 160° \le \alpha_F \le 200° \end{matrix} \tag{50}$$

$$Y_{VF} = k_2u_F^2 + F_1v_F|v_F| \qquad 20° < \alpha_F < 160° \tag{51}$$

$$Y_{VF} = -k_2u_F^2 + F_1v_F|v_F| \qquad 200° < \alpha_F < 340° \tag{52}$$

$$N_{VF} = -Y_{VF}\ell_{VF} \tag{53}$$

Horizontal Stabilizer Aerodynamics

$$w_H = w_B + \frac{\lambda}{R_7} + u_B\delta_s + \ell_{HS}q_B + w_C \tag{54}$$

$$u_H = u_B \tag{55}$$

The horizontal stabilizer of the helicopter is connected to the longitudinal cyclic control and varies in a nonlinear manner with longitudinal cyclic stick position (table 1).

At the time these equations were developed, data for the UH-1H stabilizer incidence schedule were not available. Since the UH-1B stabilizer is linked in a similar manner to the cyclic controls, and table 1 values were available, they were used in lieu of UH-1H values.

$$\sin \alpha_{HS} = \frac{w_H}{\left(u_H^2 + w_H^2\right)^{1/2}} \tag{56}$$

$$Z_H = -H_1 w_H u_H - H_4 w_H |w_H| \qquad \begin{matrix} -20° \le \alpha_{HS} \le 20° \\ 160° \le \alpha_{HS} \le 200° \end{matrix} \tag{57}$$

$$Z_H = -H_2 u_H^2 - H_4 w_H |w_H| \qquad 20° < \alpha_{HS} < 160° \tag{58}$$

$$Z_H = H_2 u_H^2 - H_4 w_H |w_H| \qquad 200° < \alpha_{HS} < 340° \tag{59}$$

$$M_H = Z_H \ell_{HS} \tag{60}$$

Total Body Forces and Moments

$$x_B = X_R + X_F \tag{61}$$

$$Y_B = Y_R + Y_{TR} + Y_F + Y_{VF} \tag{62}$$

$$Z_B = Z_R + Z_F + Z_H \tag{63}$$

$$L_B = L_R + L_{TR} \tag{64}$$

$$M_B = M_R + M_F + M_H \tag{65}$$

$$N_B = N_R + N_{TR} + N_F + N_{VF} \tag{66}$$

The form of the equations for the fuselage, horizontal stabilizer and vertical fin aerodynamics results from using trigonometric functions to approximate the lift and drag curves in wind axes, and then resolving these forces and relative wind into body axes.

Estimation of Rotor Flapping with Respect to the Shaft

The tip path plane orientation with respect to the control axis is represented by the values of the flapping coefficients a_1 and b_1. As an approximation to the actual rotor flapping angle with respect to the shaft a_{1S} and b_{1S}, the following equations were used. They reflect the influences of the cyclic control inputs A_{1C} and B_{1C} and the computed flapping amplitudes a_1 and b_1. The sign convention of reference 5 is followed.

$$a_{1s} = a_1 - b_{1sw} \tag{67}$$

$$b_{1s} = b_1 + a_{1sw} \tag{68}$$

$$a_{1sw} = \phi_c \cos \phi_t \frac{v_C}{\left(u_C^2 + v_C^2\right)^{1/2}} - \phi_c \sin \phi_t \frac{u_C}{\left(u_C^2 + v_C^2\right)^{1/2}} \tag{69}$$

$$b_{1sw} = -\phi_c \sin \phi_t \frac{v_C}{\left(u_C^2 + v_C^2\right)^{1/2}} - \phi_c \cos \phi_t \frac{u_C}{\left(u_C^2 + v_C^2\right)^{1/2}} \tag{70}$$

$$\phi_c = \cos^{-1}\left(\cos A_{1C} \cos B_{1C}\right) \tag{71}$$

$$\phi_t = \tan^{-1}\left(\frac{\tan A_{1C}}{\sin B_{1C}}\right) \tag{72}$$

The maximum flapping amplitude is given by

$$\beta_m = \left(a_{1s}^2 + b_{1s}^2\right)^{1/2} \tag{73}$$

where β_m is the maximum teetering angle with respect to the rotor mast. The orthogonal components of flapping in the wind-shaft axis system are a_{1s} and b_{1s}, and ϕ_c and ϕ_t are the amplitude of the cyclic input and the phase of the cyclic input, respectively.

COMPARISON OF HELICOPTER FLIGHT DYNAMICS WITH MATH MODEL DYNAMICS

A Bell UH-1H helicopter was instrumented and flown at Crows Landing NAS November 12, 1974 for the purpose of obtaining flight records against which the simulator model could be compared.

In this section, the helicopter responses to step control inputs are compared directly with the math model responses to the same inputs.

Flight Conditions

Two flight conditions are shown: hover out of ground effect and 60 knots level flight. The flight tests were made at nominally sea level no-wind conditions. The simulator model is shown at standard day, sea level conditions.

Control Inputs

Step control inputs of from ±1.25 cm to ±2.5 cm (±1/2 in. to ±1 in.) were made in collective, pitch, roll, and yaw controls. The pilot was instructed to establish a steady flight condition (zero rate of climb, pitch, roll, and yaw) and then to input and hold the appropriate control for as long a period as possible before initiating a recovery. These inputs are simulated as true steps in the simulator time history comparisons. Amplitudes for the simulator inputs are adjusted to conform as closely as possible to the flight values for linear displacements at the pilot's hand or foot.

Aircraft Configuration

The aircraft flown, and the simulator model, represents a standard UH-1H (with stabilizer bar) weighing 2800 kg (6158 lb). This weight is the estimated initial gross weight of the helicopter at the commencement of the tests. Both the weight and longitudinal center of gravity were derived from a pre-flight weight and balance of the helicopter, followed by adjustments for fuel burnoff and personnel transfers prior to the test runs.

The inertia values used for the simulator model are representative values obtained from unpublished Bell Helicopter Company data.

The vertical center of gravity of the helicopter was not known. The characteristic lengths used in the model reflect only a reasonable estimate of its value.

Aircraft On-Board Sensors

The sensors on the aircraft were:

1. Body angular rate gyros sensing roll rate, pitch rate and yaw rate,

2. Vertical gyro sensing Euler attitudes of the aircraft in roll, pitch, and heading,

3. Body accelerometers measuring body axis accelerations,

4. Airspeed indicator,

5. Instantaneous vertical speed indicator (IVSI), i.e., rate-of-climb pressure instrument,

6. Sensors for measuring control displacements at the pilot's hand or foot: δ_c (collective pitch stick), δ_e (longitudinal cyclic stick), δ_a (lateral cyclic stick), and δ_p (pedal, or θ_{TR} pitch input).

Time History Comparisons

The aircraft and model angular rate and attitude responses to the step control inputs are shown opposite each other in figures 2 through 9. Figures 2 through 5 are responses to inputs initiated from a steady 60 knot trimmed forward flight condition. Figures 6 through 9 are responses to inputs starting from an initial trimmed hover condition.

The format for each figure is the same. The first page consists of p_B, q_B and r_B versus time for the control input shown at the bottom of the page. The second page shows the displacement angles ϕ, θ and ψ and the vertical acceleration A_z for the same control input. Vertical lines on the flight data denote the beginning and end of the control input. Tick marks on the model data indicate control input. All pens are zeroed at the end of the control step on the model data.

The aircraft A_z is included only for a general trend comparison since the filtering of this signal was subsequently found to be questionable. The aircraft IVSI was suspected of having a large lag since radar height position data did not compare well with integrated instantaneous vertical speed indicator (IVSI) readings. Consequently, a comparison of rate-of-climb response to collective pitch is not shown. Comparison with radar height data in hover did show that the rate-of-climb response is a first order type of heave response ($h = K_h \delta_c (1 - e^{-t/\tau_{\dot{h}}})$) and that both the time constant and steady state values were well modeled by the equations.

A direct comparison of the records at 60 knots shows that the primary responses to the control inputs are reasonably well modeled: pitch rate to longitudinal cyclic, roll rate to lateral cyclic and yaw rate to a pedal step. The coupled responses to these same steps show sign differences in some cases, but the absolute magnitudes of the responses are small. For the pedal step and the collective step, where the coupled responses are larger, the magnitudes and signs of the coupled responses appear to be properly represented.

Attempts to duplicate flight responses in hover were not as successful. The primary responses are sufficiently well modeled so that the pilot was given proper cues in the first one to two seconds following a servo failure. The long term response in pitch rate is exaggerated and the long term response in roll rate is underpredicted by the model. In addition, strong pitch coupling is evident in the flight records for both the lateral step input and the pedal step input, a phenomenon not present in the model. The physical reason for these coupled responses was not understood.

The primary yaw rate response in hover is good. The coupled yaw responses to lateral cyclic pitch and to collective pitch are satisfactory.

The validation effort was stopped at this point because further attempts to improve the hover responses were not successful, or it changed the model adversely at 60 knots. Without more insight into the basic aerodynamics of the aircraft in hover, it was also difficult to understand how to alter the equations to obtain the desired results.

The initial responses to servo hardovers were believed realistic enough to provide the pilot with the appropriate cues to initiate recovery. The overall dynamics appeared to be adequate to give a reasonable estimate of aircraft excursions during the recovery from a failure.

Pilot Evaluations

In addition to comparing the model with flight time histories, the model was operated both in a fixed-base simulator and in a six-degree-of-freedom moving-base simulator (6 DOF). The model was flown with and without motion washout in hover, and with motion washout at 60 knots. The flights without washout were made with open cab and with real outside-world references. The flights with washout, and fixed base, were made with visual reference provided by a terrain model.

The model was judged to be realistic at 60 knots by the research pilots who flew the simulation. However, the model was judged to be difficult to fly normally in hover by every pilot who flew it. Precise hover and precise maneuvers around hover at low speeds, including quick stops and lateral translations, were more difficult with the simulated model than with the actual helicopter. Motion cues provided by the 6 DOF simulator did not change the pilot's evaluations.

In spite of this, all pilots were able to adapt themselves to the simulator and fly quite precisely after a learning period. Precision hover in the 6 DOF simulator with open cab and no motion washout was possible. In addition to this, recoveries from roll and pitch servo hardovers were accomplished, and a precision hover reestablished within the 5.5 m^2 of possible simulator travel.

This model was used in a flight control simulation described in reference 1.

CONCLUDING REMARKS

The mathematical model of a UH-1H helicopter described in this report was developed for real time piloted simulation. The model was evaluated by comparing its dynamics objectively with flight test results and subjectively with pilot evaluations. The model appears to be satisfactory for flying qualities investigations at forward speeds and usable, but less realistic, for hover. The reasons for the discrepancies between flight and simulation have not yet been determined.

It is believed that enough information has been provided here to enable a potential user to decide whether the model is suitable for his application.

REFERENCES

1. Corliss, Lloyd C.; and Talbot, P. D.: A Failure Effects Simulation of a Low Authority Flight Control Augmentation System on a UH-1H Helicopter. NASA TM-73,258, 1977.

2. McFarland, R. F.: A Standard Kinematic Model for Flight Simulation at NASA-Ames. NASA CR-2497, 1975.

3. Seckel, Edward; and Curtiss, H. C., Jr.: Aerodynamic Characteristics of Helicopter Rotors. Rotor Contributions to Helicopter Stability Parameters. Princeton University Report, 1963.

4. Biggers, J. C.; McCloud, J. L., III; and Patterakis, Peter: Wind Tunnel Tests of Two Full Scale Helicopter Fuselages. NASA TN D-1548, 1962.

5. Gessow, A.; and Myers, G. C., Jr.: Aerodynamics of the Helicopter. Macmillan, 1952.

6. Flanigen and Porter: Category II Performance Tests of the YUH-1D with a 48-foot Rotor. AFFTC TDR 64-27, Nov. 1964.

7. Wilcock, T.; and Thorpe, A. C.: Flight Simulation of a Wessex Helicopter: A Validation Exercise. RAE TR 73096, Sept. 1973.

8. McCloud, J. L., III; Biggers, J. C.; and Stroub, R. H.: An Investigation of Full Scale Helicopter Rotors at High Advance Ratios and Advancing Tip Mach Numbers. NASA TN D-4632, 1968.

9. Finnestead, R. L.; and Graham, W. A.: Tail Rotor Performance and Translational Flight Handling Qualities Tests of the UH-1H Helicopter. USAASTA Project #71-18, Jan. 1972.

TABLE 1.- VARIATION OF HORIZONTAL STABILIZER INCIDENCE

WITH LONGITUDINAL STICK POSITION

δ_e, cm	δ_e, in.	δ_s, rad
16.38	-6.45	0.0224
15.25	-6.00	.0174
12.7	-5.00	0
10.16	-4.00	-.0192
7.62	-3.00	-.0384
5.08	-2.00	-.0541
2.54	-1.00	-.0690
0	0	-.0820
2.54	1.00	-.0850
5.08	2.00	-.0803
7.62	3.00	-.0628
10.16	4.00	-.0300
12.7	5.00	.0035
15.25	6.00	.0593
16.38	6.45	.0942

TABLE 2.- SUMMARY OF UH-1H PHYSICAL CONSTANTS

	English	Metric
Main rotor		
Hub precone angle	2.75 deg	
Radius	24.13 ft	7.35 m
Chord	1.75 ft	.53 m
Tip speed (ΩR)	760 ft/sec	231.6 m/sec
Hub station	133.5	
Hub waterline	136.5	
Solidity	.046	
Tail rotor		
Radius	4.25 ft	1.29 m
Chord	.70 ft	21.33 cm
Tip speed	740 ft/sec	225.5 m/sec
Shaft station	479.4	
Shaft waterline	137.5	
Solidity	.105	
Center of gravity		
Most forward	sta. 130	
Most aft	sta. 144	
Vertical	w.l. 55	
Horizontal stabilizer		
Area	16.4 ft^2	1.52 m^2
Span	8.75 ft	2.67 m
1/4 c station	380	
Vertical fin		
Area	12 ft^2	1.11 m^2
Span	4.5 ft	1.37 m
1/4 c station	460	
a.c., waterline	112	
Fuselage		
fe_1	19.2 ft^2	1.78 m^2
$C_{L\alpha}$ (includes stab.)	.036/deg	
$C_{m\alpha}$ (includes stab.)	0	
$C_{L\alpha}$ (no horiz. stab.)	.02/deg	
$C_{m\alpha}$ (no horiz. stab.)	7.5×10^{-3}/deg	
S_{ref}	48 ft^2	4.46 m^2
ℓ_{ref}	39 ft	3.62 m
Mast tilt	+5 deg fwd.	
Control travels (full throw)		
Collective stick	11 in.	27.9 cm
Longitudinal stick	12.9 in.	32.8 cm
Lateral stick	12.6 in.	32.0 cm
Pedals	6.9 in.	17.5 cm
Lateral cyclic rigging	2° left	
Longitudinal cyclic pitch	+12°	
Lateral cyclic pitch	+9° to -11°	
Tail rotor collective pitch		
Full l. pedal	18°	
Full r. pedal	-10°	

TABLE 3.- SUMMARY OF CONSTANTS USED IN UH-1H SIMULATION

Constant	Equation/origin	Source	Simulation value	
			English	Metric
R_1	$\frac{\sigma a}{2} \rho_o A(\Omega R)^2$	Ref. 3	3.84×10^5 lb	17.1×10^5 N
R_2	$1/4\Omega$	Ref. 3	7.37×10^{-3} sec	7.37×10^{-3} sec
R_3	$1/2$ a	Ref. 3	8.70×10^{-2}	
R_4	$1/\Omega$	Ref. 3	2.95×10^{-2} sec	2.95×10^{-2} sec
R_5	$1/4$ a	Ref. 3	4.36×10^{-2}	
R_6	$16/\gamma\Omega$	Ref. 3	.144 sec[a]	.144 sec
R_7	$1/\Omega R$	Ref. 3	1.22×10^{-3} sec/ft	4.00×10^{-3} sec/m
R_8	$[2\rho_o A(\Omega R)^2]^{-1}$	Ref. 3	1.715×10^{-7} 1/lb	$.38\times10^{-7}$ 1/N
R_9	$\frac{\sigma a}{2} \rho_o A(\Omega R)^2 R$	Ref. 5	9.107×10^6 ft-lb	12.35×10^6 J
δ_o	Mean blade drag coeff. of blade section @ zero lift		.009	
δ_2	$0.3\left[\frac{6}{\rho_o A(\Omega R)^2 \sigma a}\right]^2$	Ref. 5	1.828×10^{-11} $1/\mathrm{lb}^2$	$.092\times10^{-11}$ $1/\mathrm{N}^2$
a_o	Hub precone angle used as mean value for a_o	Ref. 8	.048 rad	.048 rad
τ_B	Constant reflects mechanical damping of stabilizer bar	Bell Helicopter Co.	3.3 sec	3.3 sec

[a] Actual value should be 0.072 based on inertia of one blade. Value used was due to an error, but was retained because subjectively more realistic handling qualities resulted.

TABLE 3.- SUMMARY OF CONSTANTS USED IN UH-1H SIMULATION - Continued

Constant	Equation/origin	Source	Simulation value	
			English	Metric
τ_R	$16/\gamma\Omega$	Same as R_6	0.144 sec[a]	0.144 sec
τ_C	Used to match flight test data	This simulation	.20 sec	.20 sec
K_B	Product of stabilizer bar linkage geometry and τ_B	Bell Helicopter Co.	$K_B = K_\ell \tau_B$ sec $K_\ell = 0.16$ Thus, $K_B = 0.528$ sec	.528 sec .528 sec
C_1	Long. cyclic/unit of stick	Ref. 9	.0324 rad/in.	.0127 rad/cm
C_4	Lateral cyclic/unit stick	Ref. 9	.0277 rad/in.	.0109 rad/cm
C_5	Collective pitch per in. of stick	Ref. 9	.025 rad/in.	.0098 rad/cm
ℓ_H	Estimated for this simulation	---	6.79 ft	2.07 m
ℓ_{TR}	Assumed constant	Ref. 9	28.0 ft	8.53 m
$X_{c.g.}$	Variable -0.520 used for sim.	Ref. 9	-.541 ft (flt. test.)	.165 m
ℓ_{VF}	Assumed constant	Ref. 9	25.0 ft	7.62 m
C_6	Tail rotor collective to pedal motion	Ref. 9	-.071 rad/in.	-.028 rad/cm
C_7	Tail rotor collective for zero pedal	Ref. 9	.119 rad	.119 rad

TABLE 3.- SUMMARY OF CONSTANTS USED IN UH-1H SIMULATION - Continued

Constant	Equation/origin	Source	Simulation value	
			English	Metric
h_{TR}	Estimated for this simulation		6.88 ft	2.10 m
ℓ_{HS}	Assumed constant	Ref. 9	19.67 ft	6.0 m
T_1	$\frac{1}{2(\Omega R)_{TR}}$	This simulation	6.76×10^{-4} sec/ft	22.17×10^{-4} sec/m
T_2	$\left[\rho_o A(\Omega R)^2\right]_{TR}^{1/2} \frac{(a\sigma)_{TR}}{8\sqrt{2}}$	This sim. (adjusted to match test).	17.0 $lb^{1/2}$	35.7 $N^{1/2}$
T_3	$\left[\rho_o A(\Omega R)^2\right]_{TR} \frac{(a\sigma)_{TR}}{6}$	This sim. (adjusted to match test).	7.0×10^3 lb	31.1×10^3 N
T_4	---	This sim. (adj. to match test).	14.9 lb/ft	217.4 N/m
T_5	---	This sim. (adj. to match test).	0	0
D_1	$\frac{1}{2}\rho_o fe_1$	Ref. 4	.022 $\frac{lb}{(ft/sec)^2}$	1.05 $\frac{N}{(m/sec)^2}$
D_2	$\frac{1}{2}\rho_o fe_2$	Estimated for this sim.	.201 $\frac{lb}{(ft/sec)^2}$	9.62 $\frac{N}{(m/sec)^2}$
D_3	$\frac{1}{2}\rho_o fe_3$	Est. for this sim.	.646 $\frac{lb}{(ft/sec)^2}$	30.92 $\frac{N}{(m/sec)^2}$
L_1	$\left(\rho_o S_{ref} C_{L_{\alpha_{FUS}}}\right)/2$	This sim. and ref. 4	6.54×10^{-2} $\frac{lb}{(ft/sec)^2}$	3.13 $\frac{N}{(m/sec)^2}$
Y_1	Assumed same as L_1		6.54×10^{-2} $\frac{lb}{(ft/sec)^2}$	.29 $\frac{N}{(m/sec)^2}$

TABLE 3.- SUMMARY OF CONSTANTS USED IN UH-1H SIMULATION - Continued

Constant	Equation/origin	Source	Simulation value	
			English	Metric
M_1	$\frac{1}{2}\rho_o S_{ref} \ell_{ref} C_{m_{\alpha_{FUS}}}$	This simulation and ref. 4	$0.956 \frac{\text{ft-lb}}{(\text{ft/sec})^2}$	$13.95 \frac{\text{J}}{(\text{m/sec})^2}$
N_1	Assumed same as L_1		$.956 \frac{\text{ft-lb}}{(\text{ft/sec})^2}$	$13.95 \frac{\text{J}}{(\text{m/sec})^2}$
H_1	$\frac{1}{2}\rho_o S_{HS} C_{L_{\alpha_{HS}}}$	Adjusted to match flt. data	$.031 \frac{\text{lb}}{(\text{ft/sec})^2}$	$1.48 \frac{\text{N}}{(\text{m/sec})^2}$
H_2	$H_1 \tan 20°$	This simulation	$.01128 \frac{\text{lb}}{(\text{ft/sec})^2}$	$.54 \frac{\text{N}}{(\text{m/sec})^2}$
H_4	$\frac{1}{2}\rho_o S_{HS} C_{D_{\alpha}} = 90°$	Adjusted to match test data	$.0083 \frac{\text{lb}}{(\text{ft/sec})^2}$	$.40 \frac{\text{N}}{(\text{m/sec})^2}$
F_1	$\frac{1}{2}\rho_o S_{FIN} C_{D_{\alpha}} = 90°$	Adjusted to match test data	$.016 \frac{\text{lb}}{(\text{ft/sec})^2}$	$.77 \frac{\text{N}}{(\text{m/sec})^2}$
k_1	$\frac{1}{2}\rho_o S_{FIN} C_{L_{\alpha_{FIN}}}$	Adjusted to match test data	$.0292 \frac{\text{lb}}{(\text{ft/sec})^2}$	$1.40 \frac{\text{N}}{(\text{m/sec})^2}$
k_2	$k_1 \tan 20°$	This simulation	$.0106 \frac{\text{lb}}{(\text{ft/sec})^2}$	$.51 \frac{\text{N}}{(\text{m/sec})^2}$
A_{1CL}	Rigging constant — lateral cyclic pitch	Adjusted to match BHG data	-.0486 rad	-.0486 rad
B_{1CL}	Rigging constant — long. cyclic pitch	Adjusted to match BHG data	.081 rad	.081 rad
G_1	Approximation to account for ground effect	Ref. 6	.28	

TABLE 3.- SUMMARY OF CONSTANTS USED IN UH-1H SIMULATION - Concluded

Constant	Equation/origin	Source	Simulation value	
			English	Metric
Weight		Measurement	6158 (valid) lb 8700 (sim) lb	27,391 N 38,698 N
I_{xx}		Bell Helicopter Co. data	2800 slug-ft^2	3795 kg-m^2
I_{yy}		Bell Helicopter Co. data	12,733 slug-ft^2	17,259 kg-m^2
I_{zz}		Bell Helicopter Co. data	10,800 slug-ft^2	14,639 kg-m^2
I_{xz}		Bell Helicopter Co. data	1480 slug-ft^2	2006 kg-m^2

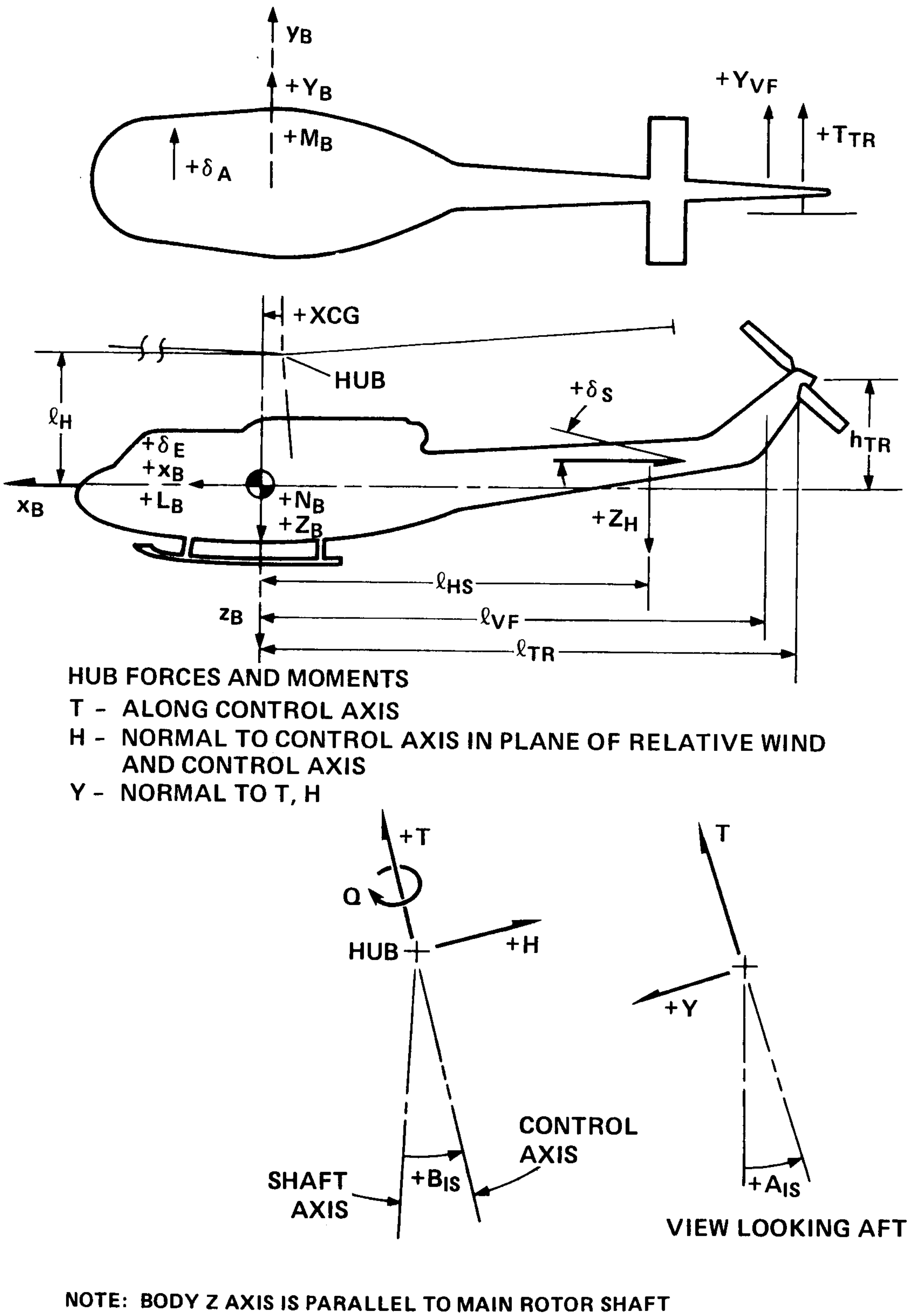

Figure 1.- Characteristic lengths and sign conventions used for forces, moments and control displacements.

AIRCRAFT	UH-1H SN AAB-11519
CONTROL INPUT	Fwd. long. step
FLIGHT CONDITION	60 knots
GROSS WEIGHT	29,371 N (6158 lb)
LONGITUDINAL CG.	

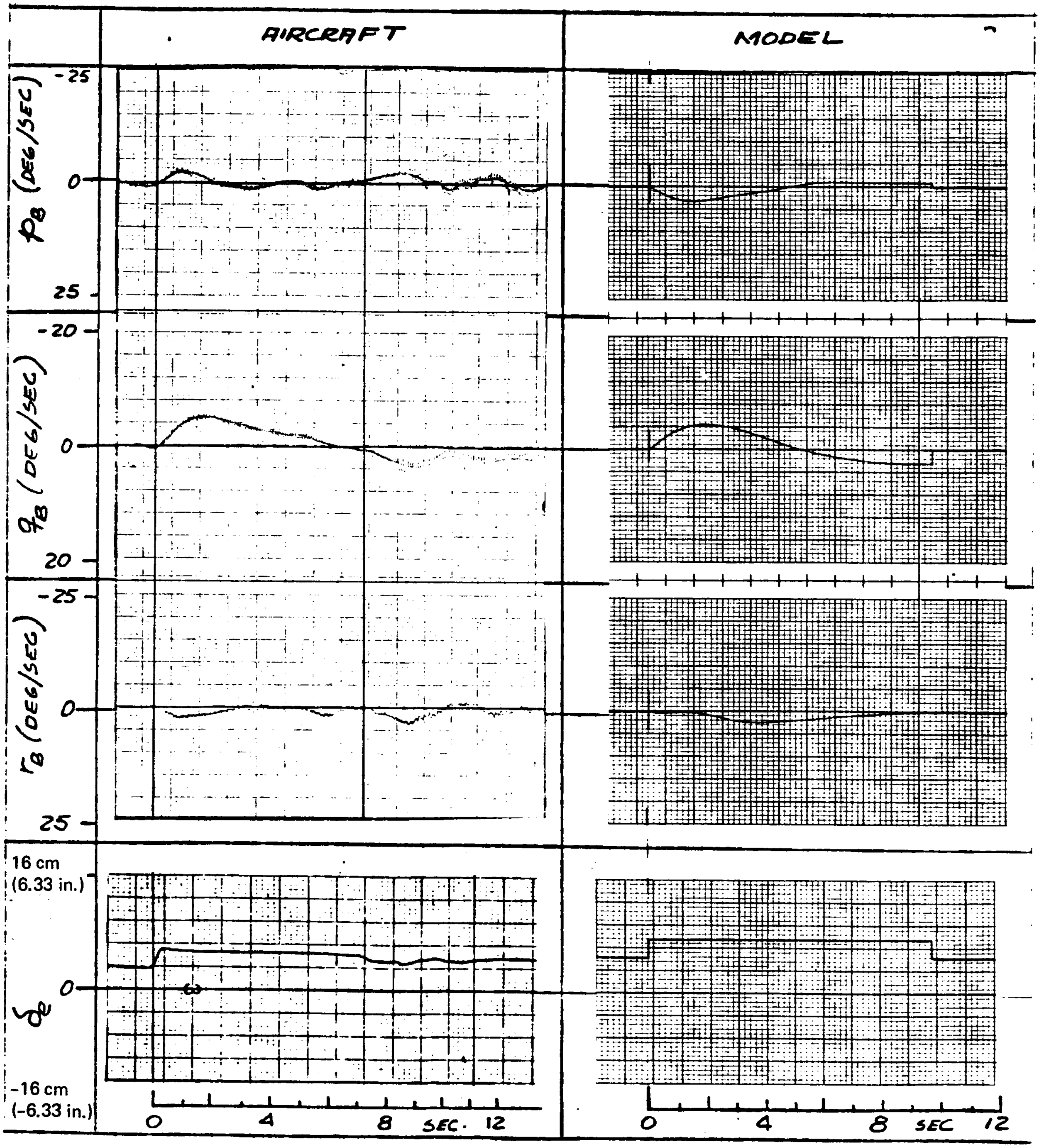

(a) Rate response.

Figure 2.- Forward cyclic step input.

60 KNOTS

CONTROL INPUT Fwd. long. step

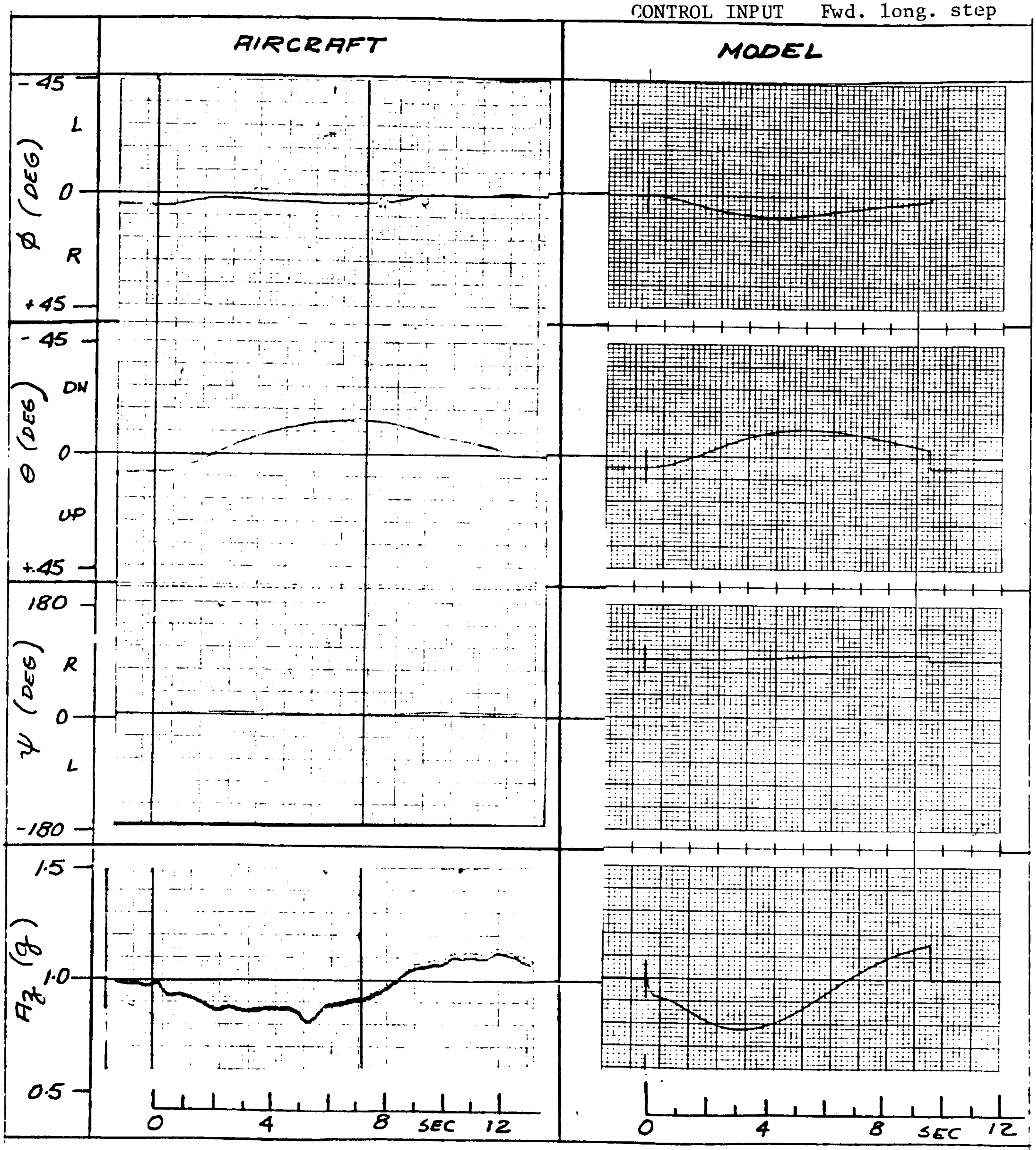

(b) Attitude response.

Figure 2.- Concluded.

CONTROL INPUT Lat. cyclic step

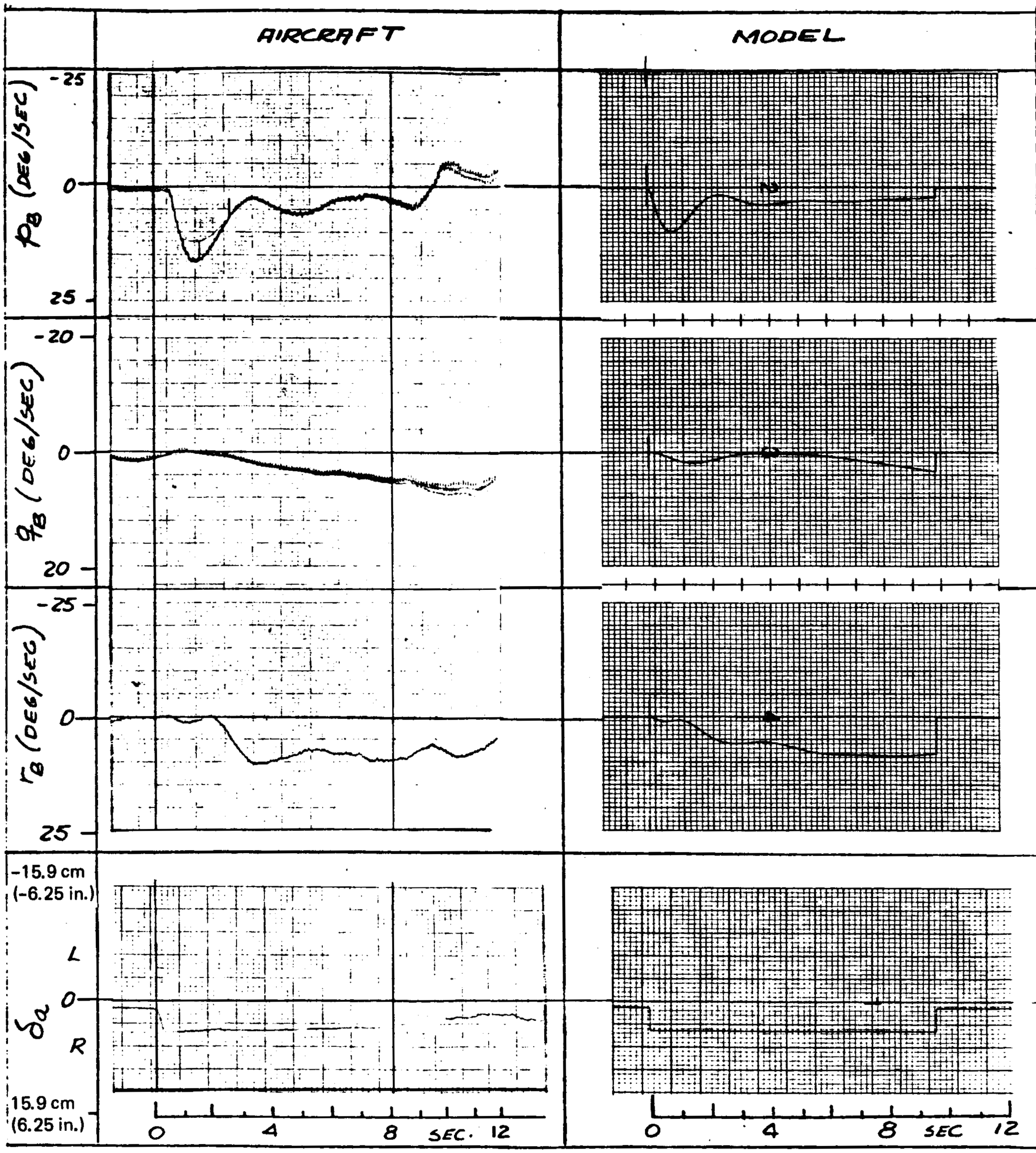

(a) Rate response.

Figure 3.- Lateral step input.

60 KNOTS CONTROL INPUT Lat. cyclic step

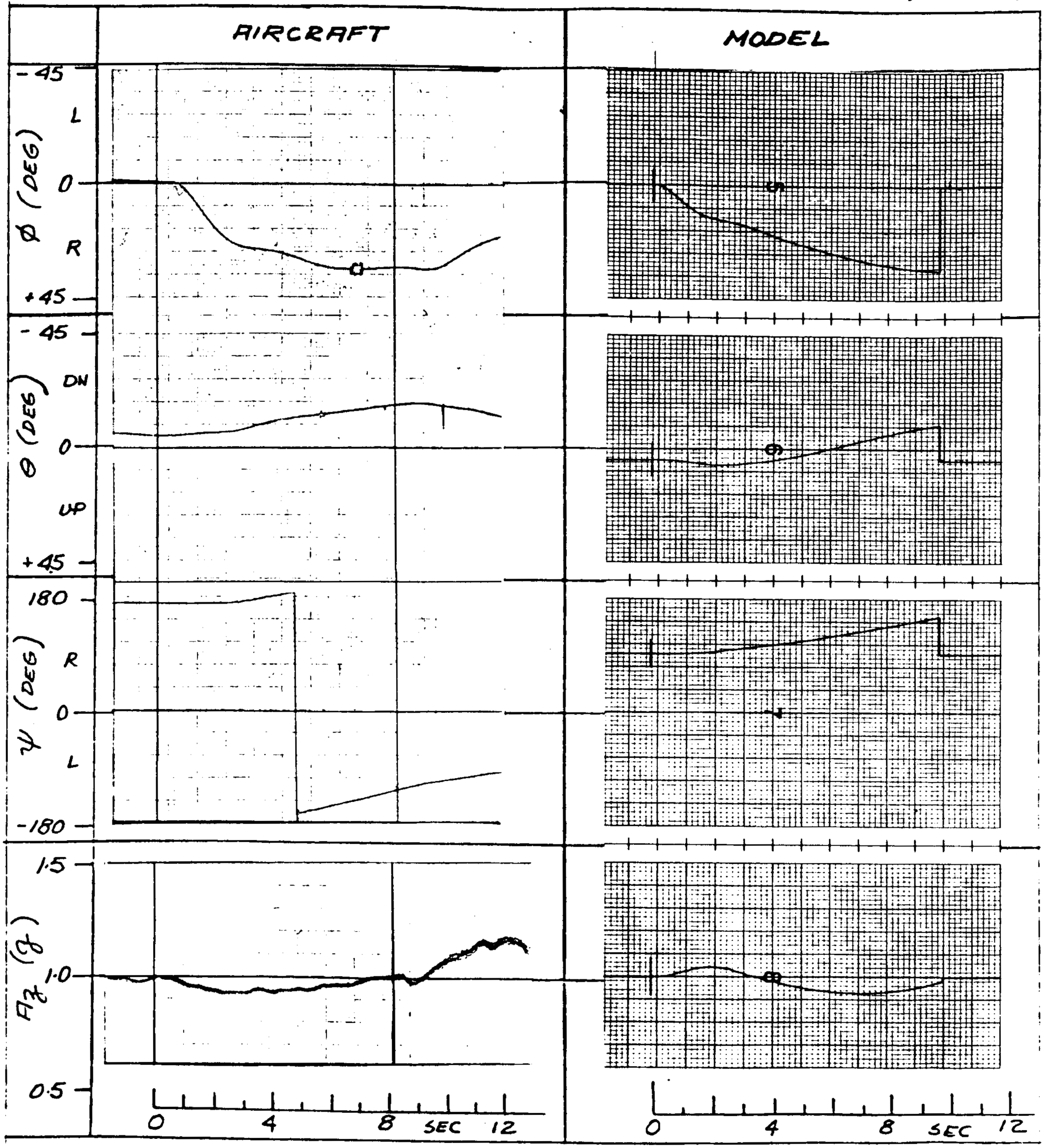

(b) Attitude response.

Figure 3.- Concluded.

60 KNOTS CONTROL INPUT R. pedal step

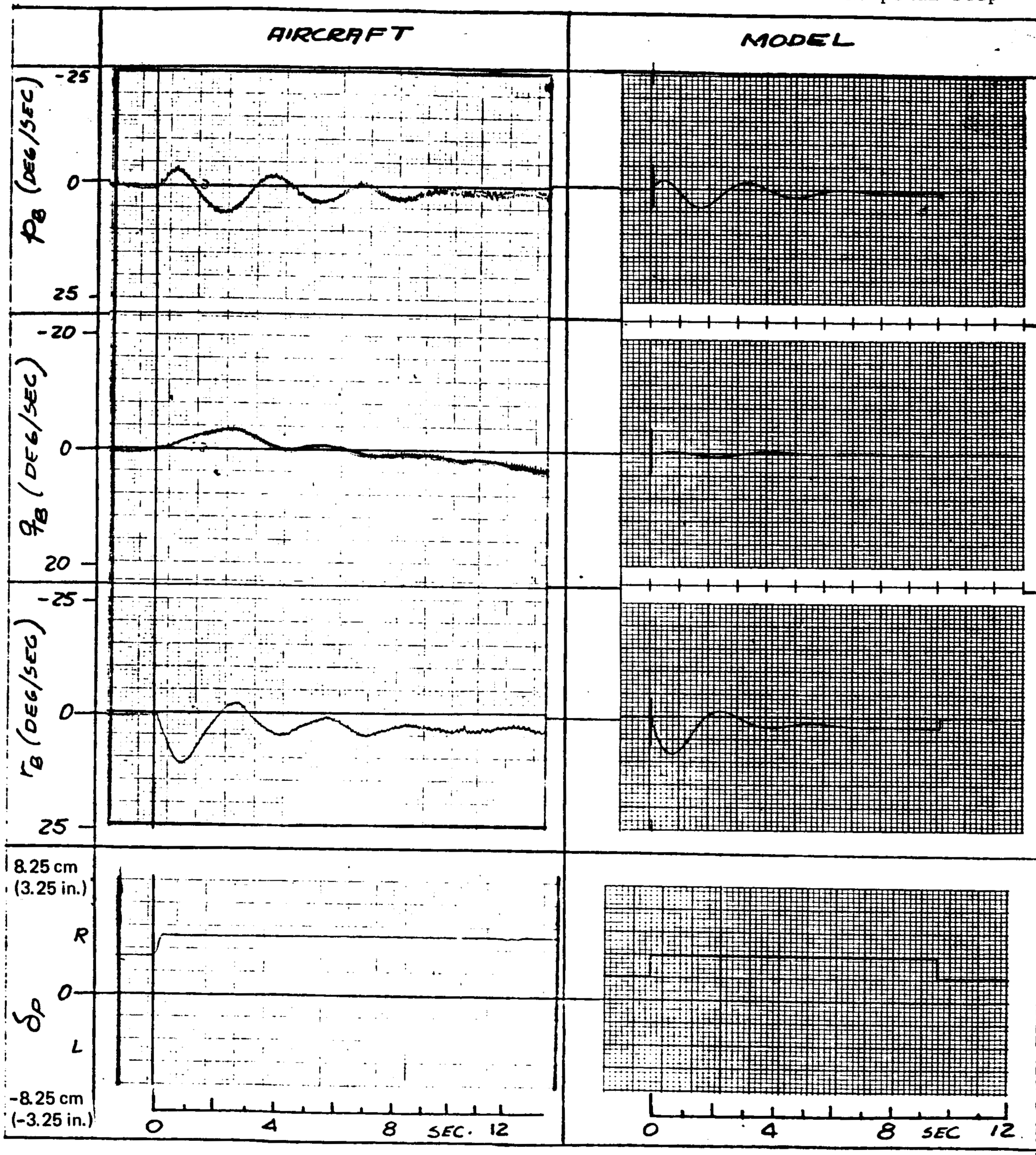

(a) Rate response.

Figure 4.- Pedal step input.

60 KNOTS

CONTROL INPUT R. pedal step

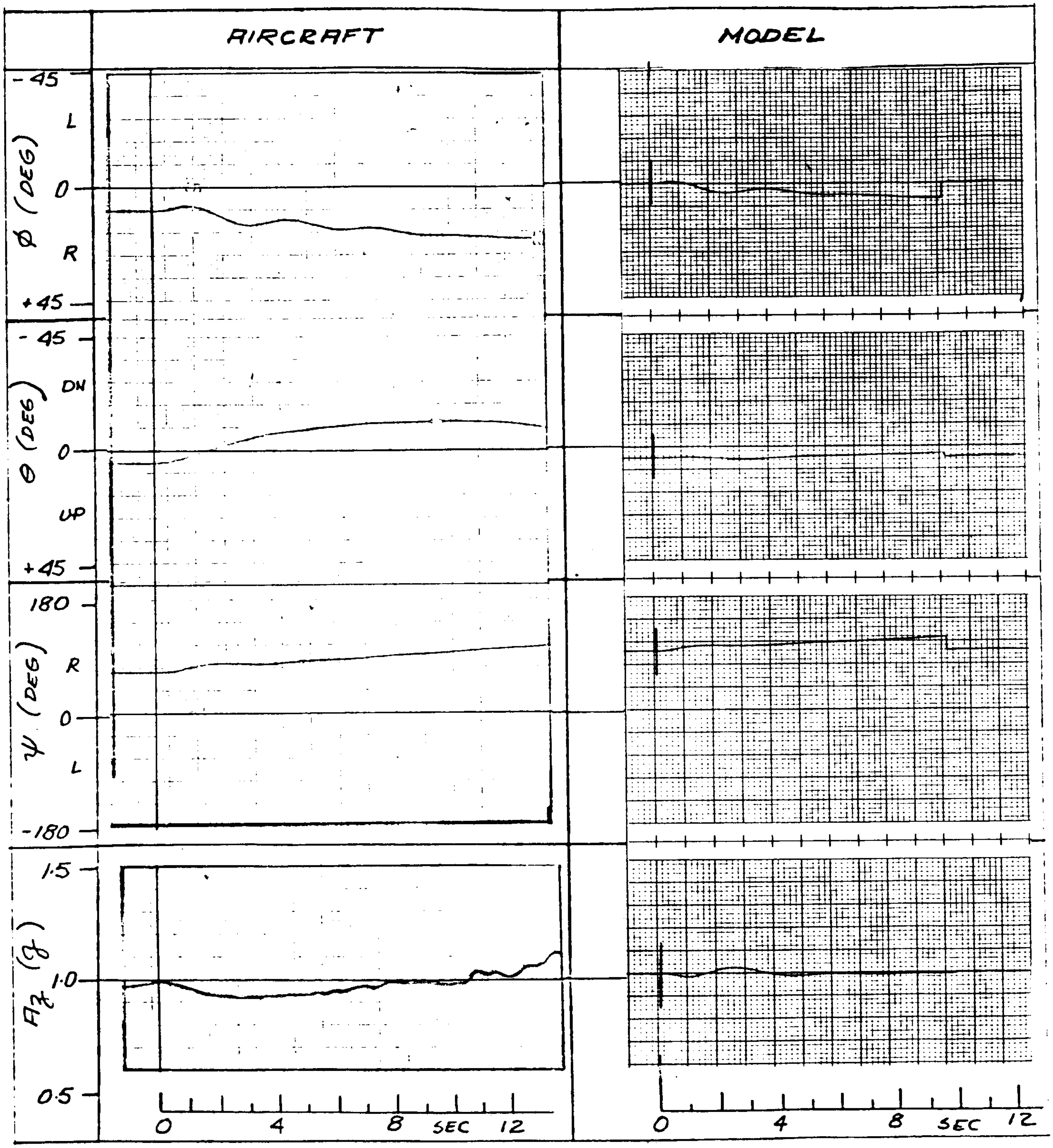

(b) Attitude response.

Figure 4.- Concluded.

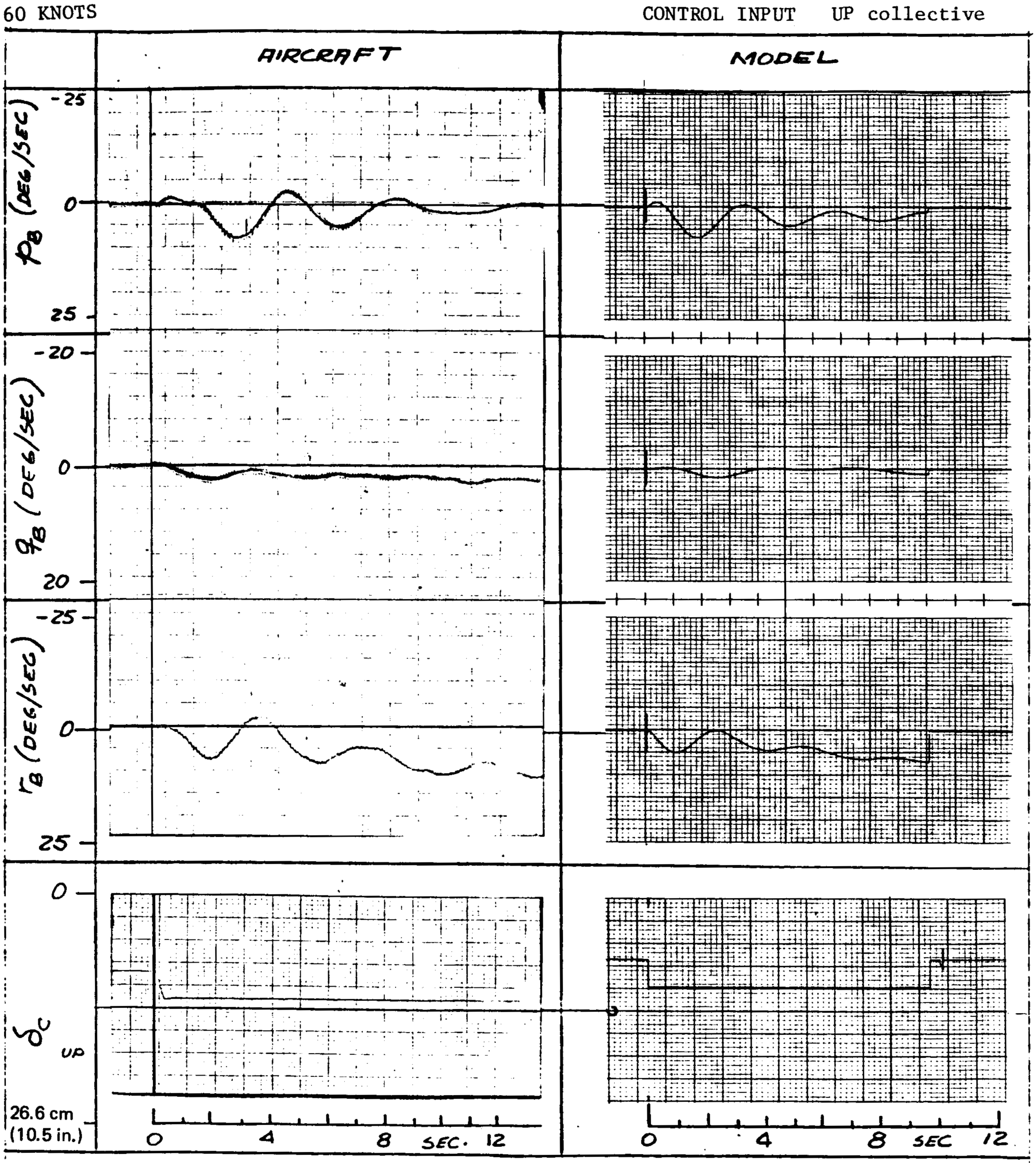

(a) Rate response.

Figure 5.- Collective step input.

60 KNOTS CONTROL INPUT UP collective

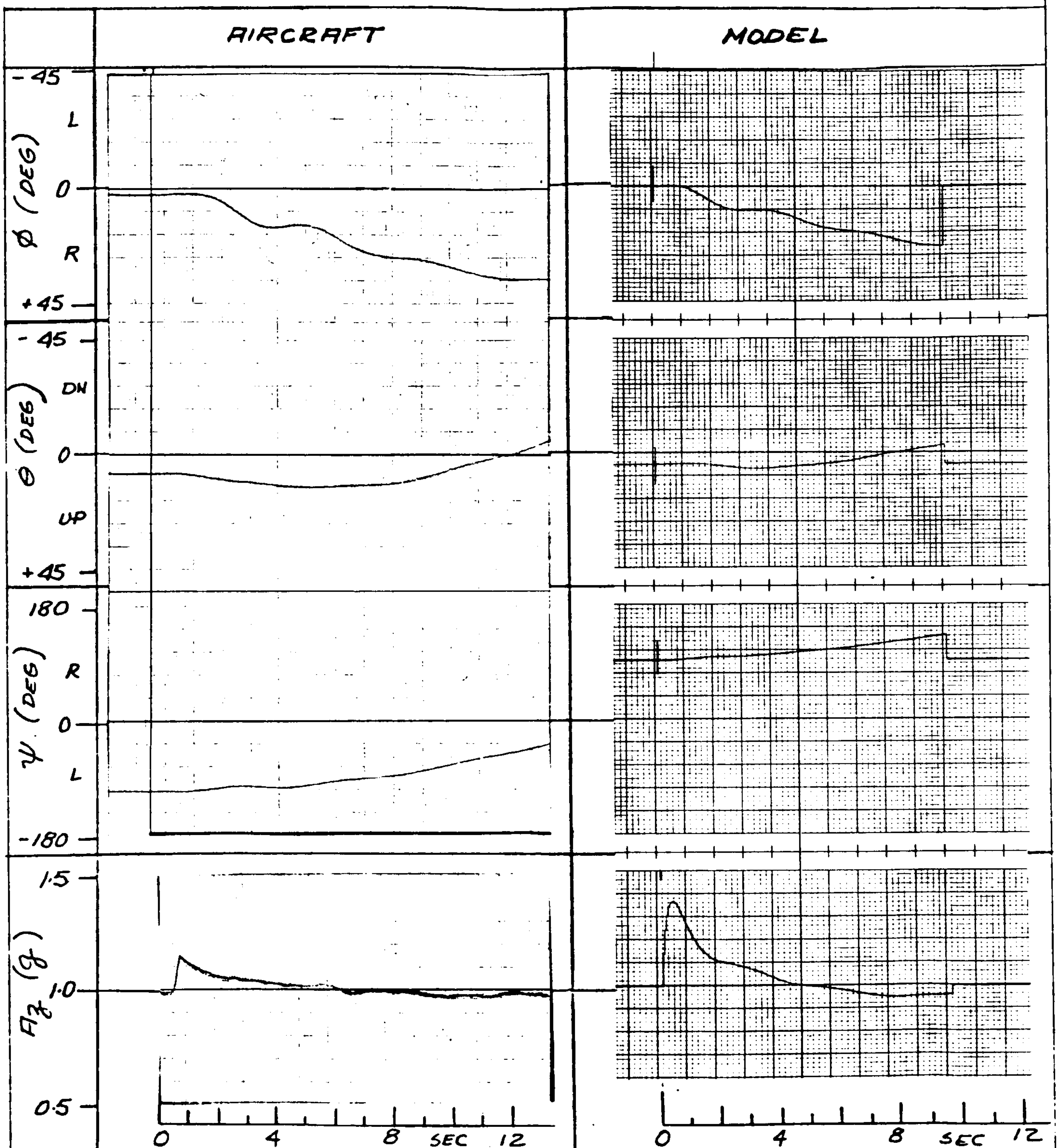

(b) Attitude response.

Figure 5.- Concluded.

AIRCRAFT	UH-1H SN AAB-11519
CONTROL INPUT	Fwd. long. step
FLIGHT CONDITION	Hover
GROSS WEIGHT	29,371 N (6158 lb)
LONGITUDINAL CG.	

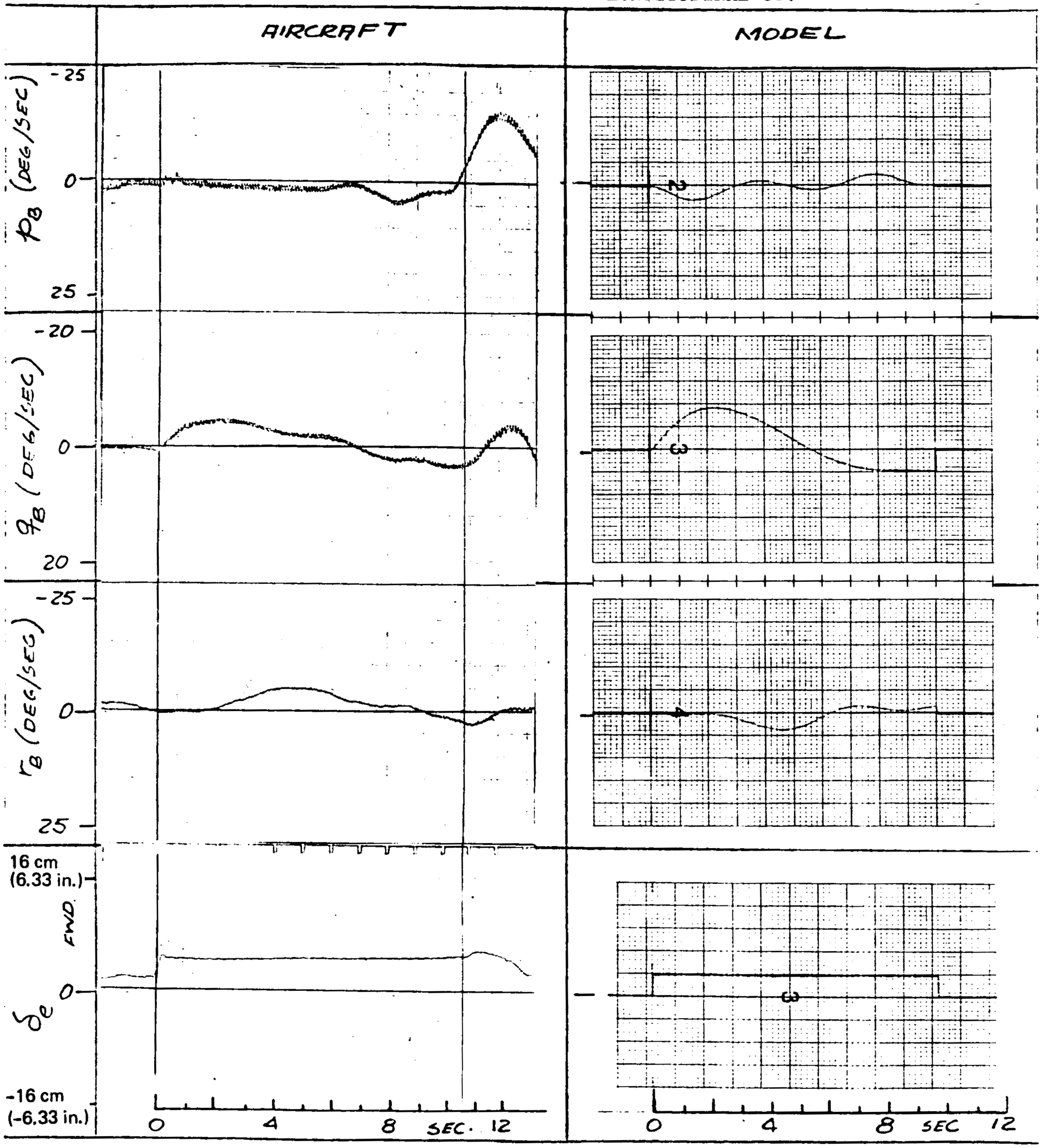

(a) Rate response.

Figure 6.- Forward cyclic step input.

HOVER

CONTROL INPUT Fwd. long. step

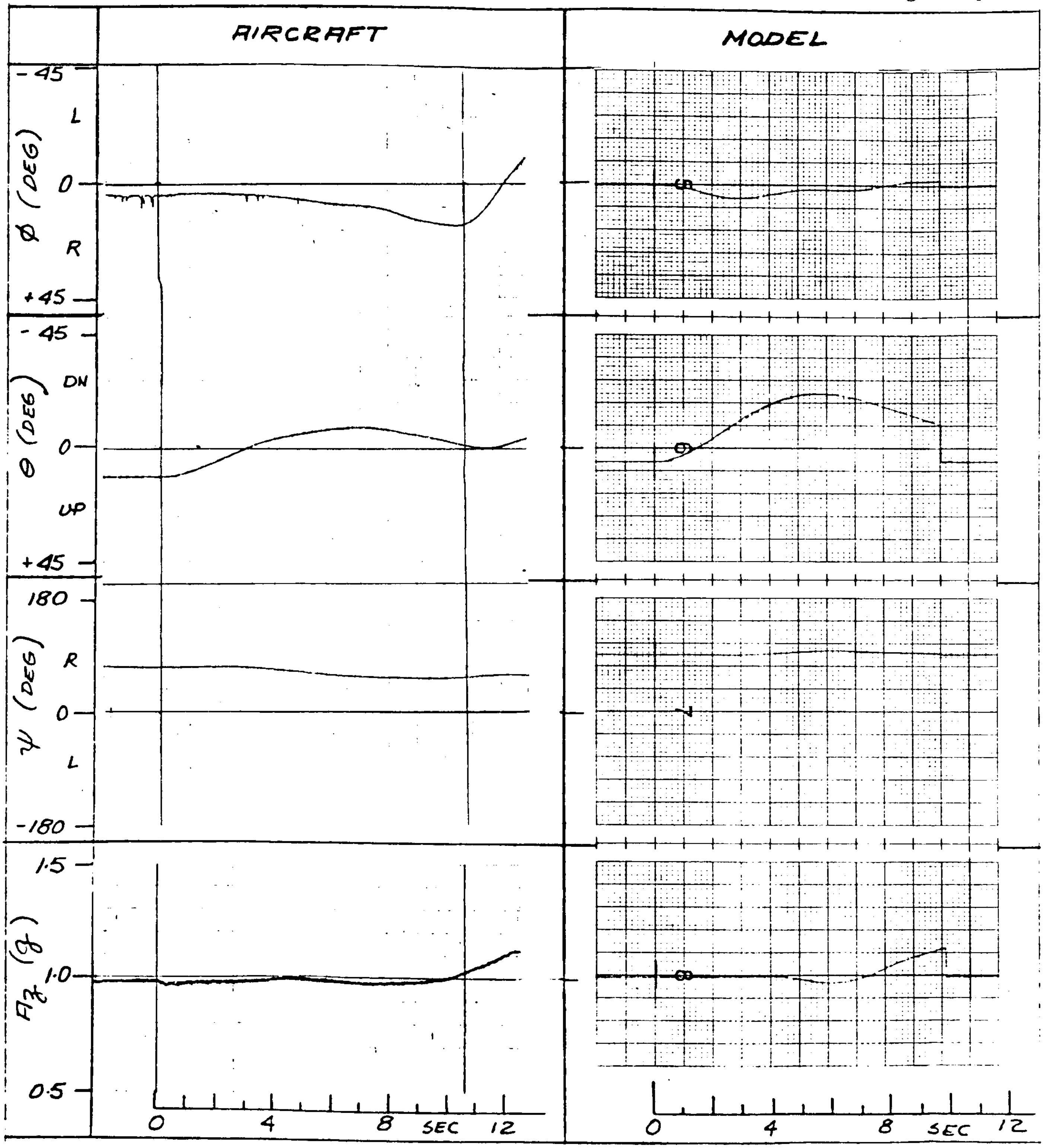

(b) Attitude response.

Figure 6.- Concluded.

HOVER CONTROL INPUT Lat. cyclic step

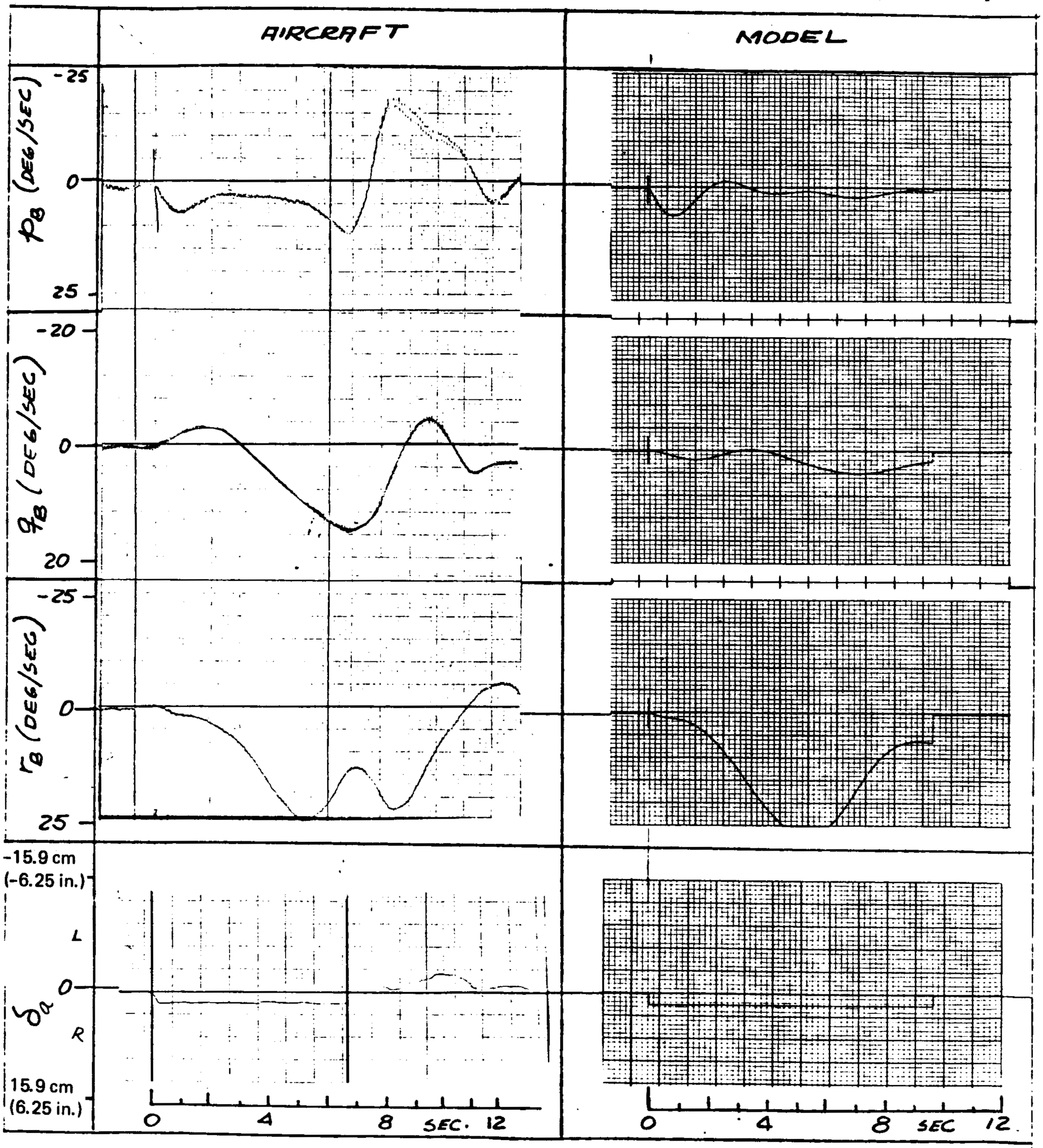

(a) Rate response.

Figure 7.- Lateral cyclic step input.

HOVER

CONTROL INPUT Lat. cyclic step

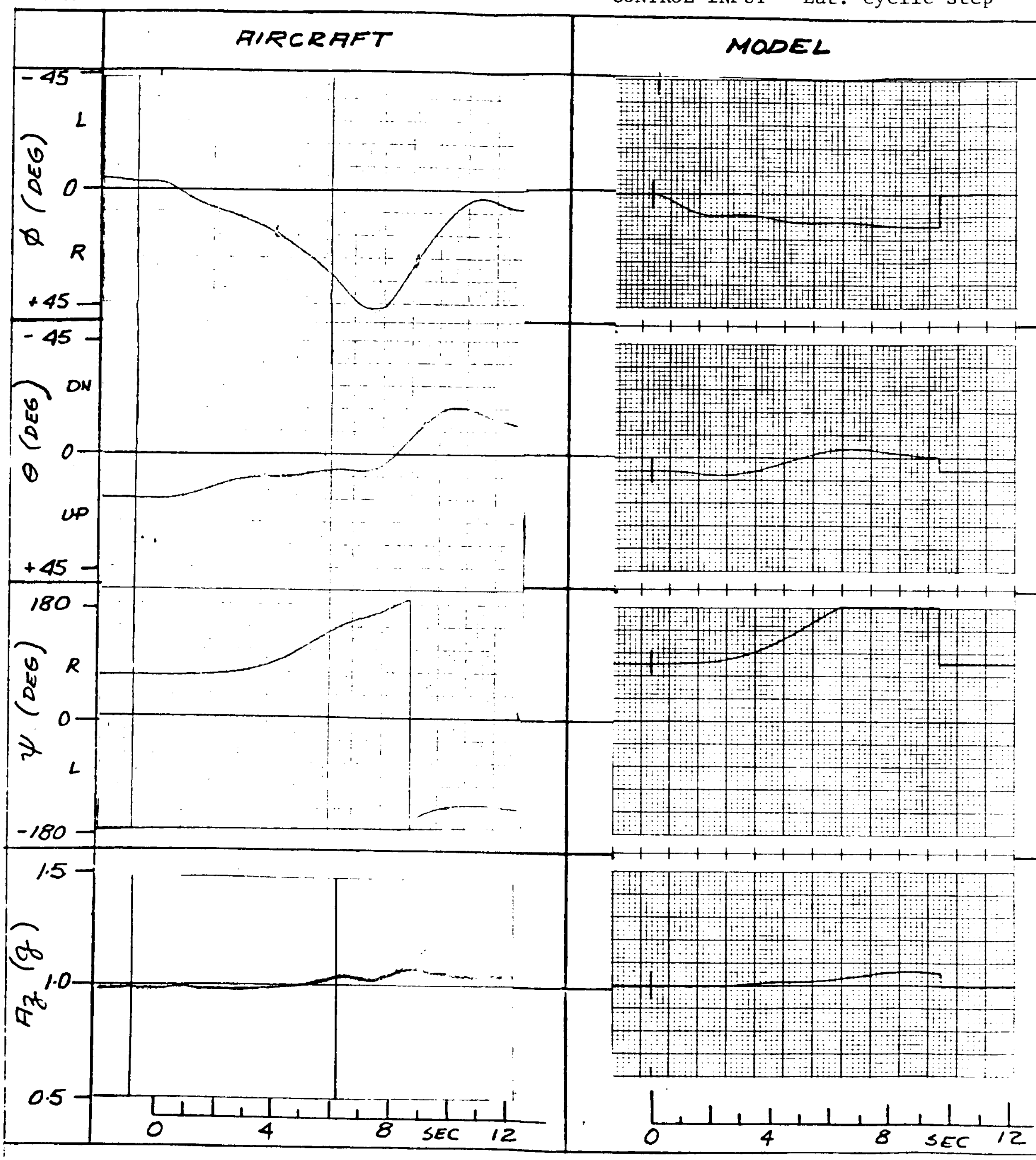

(b) Attitude response.

Figure 7.- Concluded.

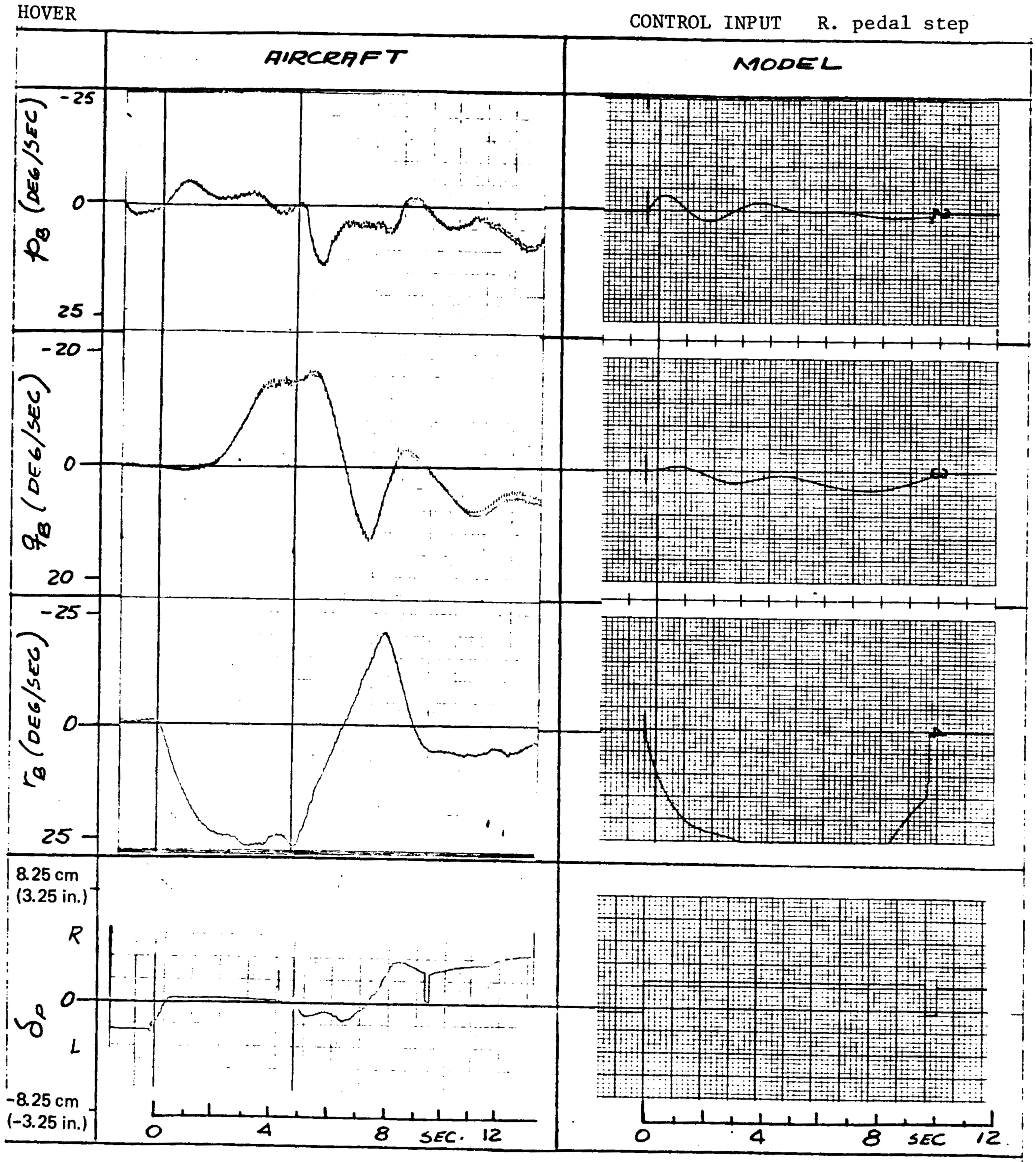

(a) Rate response.

Figure 8.- Pedal step input.

HOVER

CONTROL INPUT R. pedal step

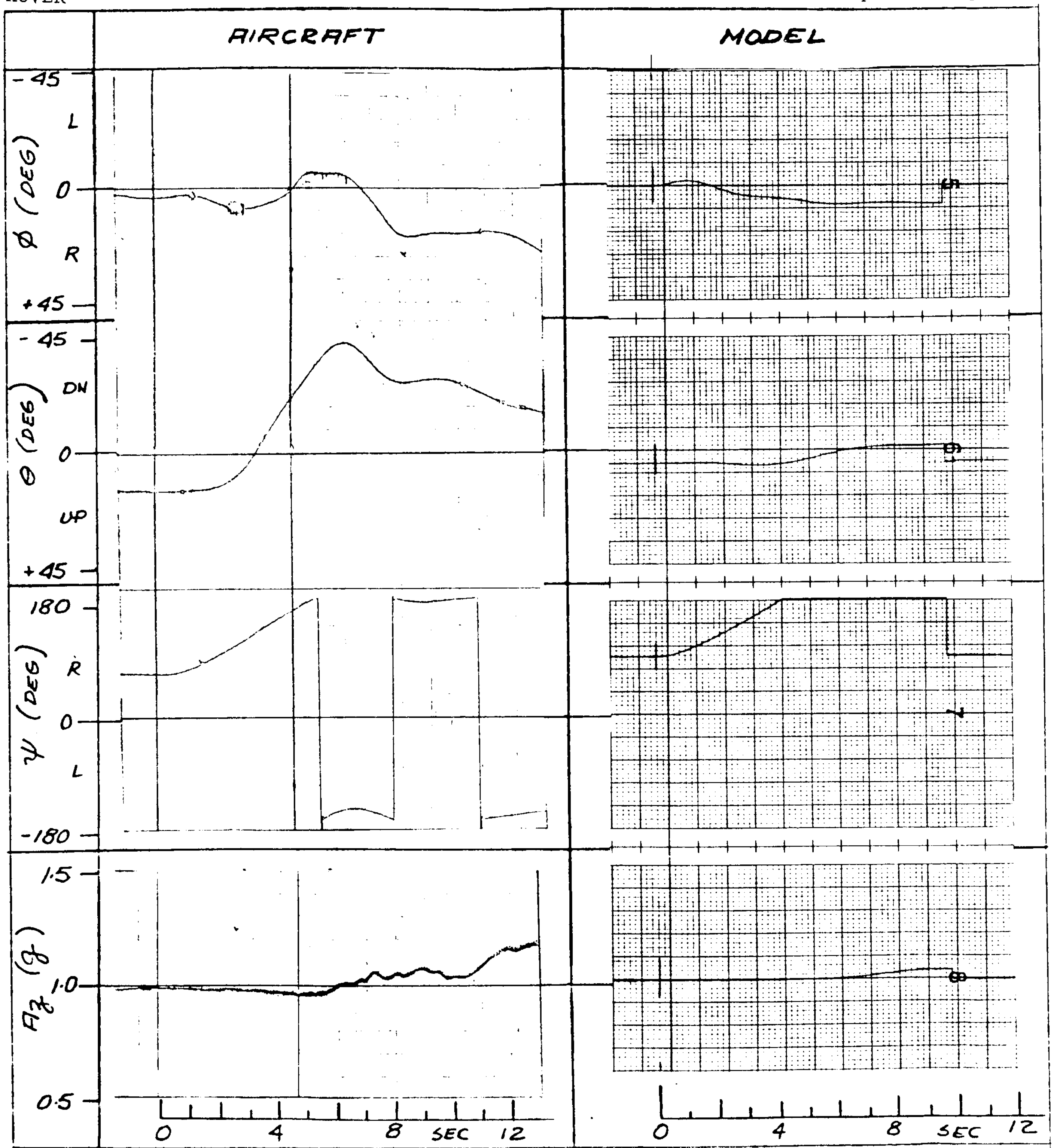

(b) Attitude response.

Figure 8.- Concluded.

HOVER

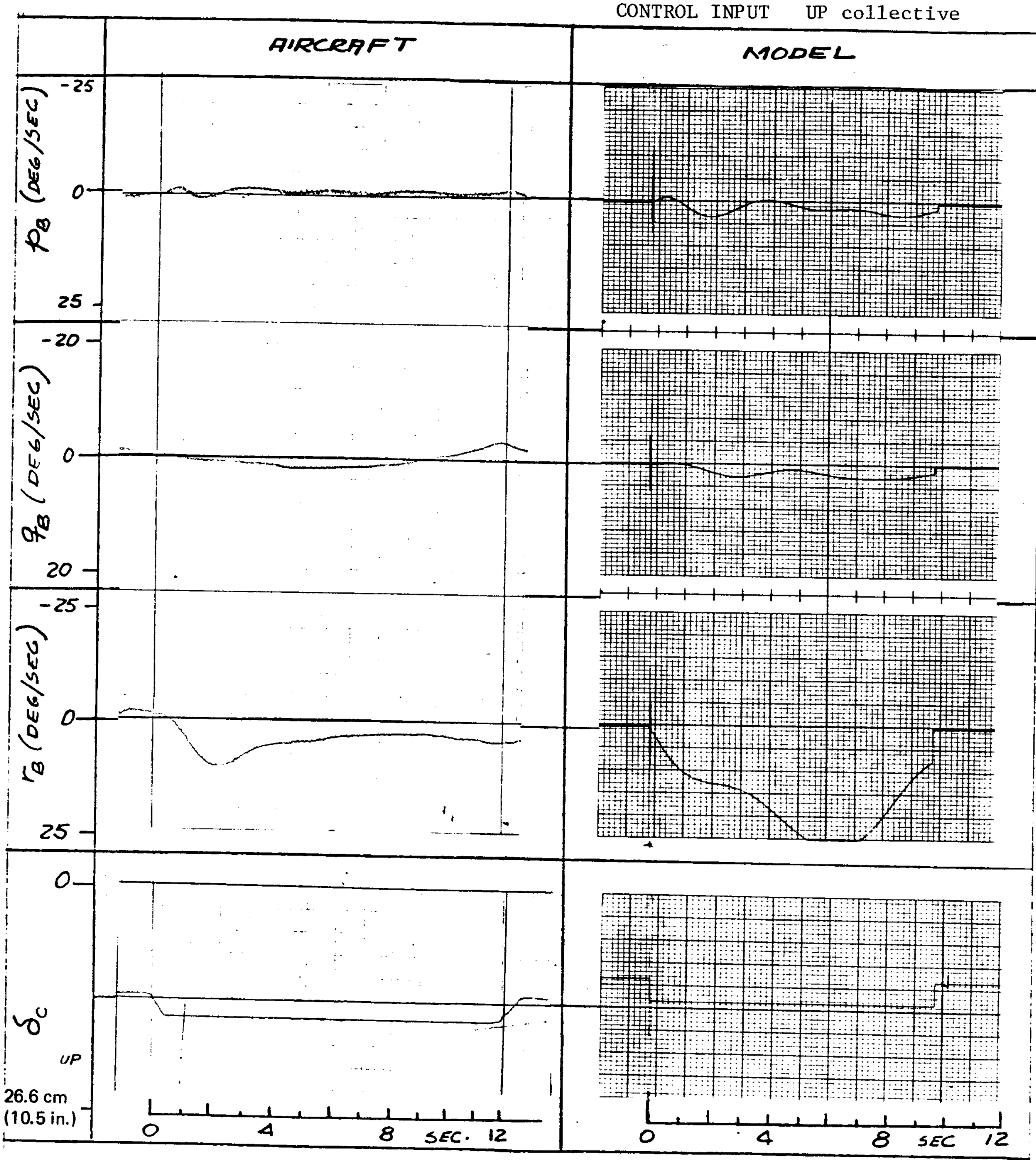

(a) Rate response.

Figure 9.- Collective step input.

Hover CONTROL INPUT UP collective

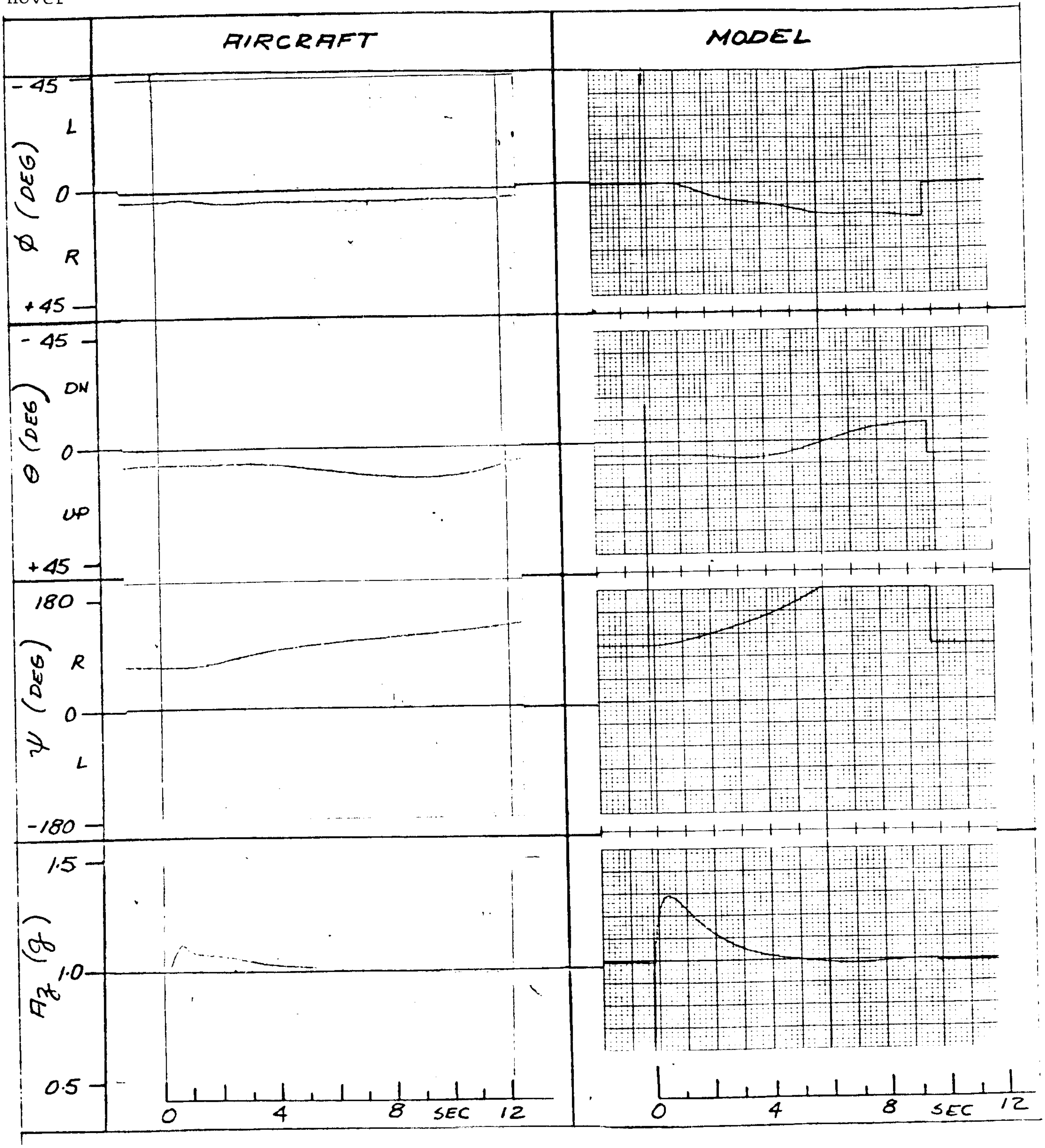

(b) Attitude response.

Figure 9.- Concluded.

1. Report No. TM-73,254	2. Government Accession No.	3. Recipient's Catalog No.
4. Title and Subtitle A MATHEMATICAL FORCE AND MOMENT MODEL OF A UH-1H HELICOPTER FOR FLIGHT DYNAMICS SIMULATIONS		5. Report Date
		6. Performing Organization Code
7. Author(s) Peter D. Talbot and Lloyd D. Corliss		8. Performing Organization Report No. A-7080
		10. Work Unit No. 505-10-23
9. Performing Organization Name and Address Ames Research Center, NASA and Ames Directorate, USAAMRDL, AVRADCOM, Ames Research Center Moffett Field, CA 94035		11. Contract or Grant No.
		13. Type of Report and Period Covered Technical Memorandum
12. Sponsoring Agency Name and Address National Aeronautics and Space Administration Washington, D. C. 20546 and U.S. Army Air Mobility R&D Laboratory, Moffett Field, CA 94035		14. Sponsoring Agency Code
15. Supplementary Notes		

16. Abstract

A model of a Bell UH-1H helicopter was developed to support several simulations at Ames Research Center and was used also for development work on an avionics system known as the V/STOLAND system at Sperry Flight Systems. This report presents the complete equations and numerical values of constants used to represent the helicopter.

Responses to step inputs of the cyclic and collective controls are shown and compared with flight test data for a UH-1H. The model coefficients were adjusted in an attempt to get a consistent match with the flight time histories at hover and 60 knots. Fairly good response matching was obtained at 60 knots, but the matching at hover was not as successful. Pilot evaluations of the model, both fixed and moving base, were made.

17. Key Words (Suggested by Author(s)) UH-1H helicopter flight dynamics; Simulation; Fixed base and comparison with flight test		18. Distribution Statement Unlimited; STAR Category — 08	
19. Security Classif. (of this report) Unclassified	20. Security Classif. (of this page) Unclassified	21. No. of Pages 45	22. Price* $3.75

*For sale by the National Technical Information Service, Springfield, Virginia 22161